J. Cell. Mol. Med. Vol 13, No 9B, 2009 pp. 3151-3173

Differential distribution of aggrecan isoforms in perineuronal nets of the human cerebral cortex

Daniela Virgintino [a], Daniela Perissinotto [b], Francesco Girolamo [a], Maria T. Mucignat [b], Luisa Montanini [d], Mariella Errede [a], Tomoyuki Kaneiwa [d], Shushei Yamada [d], Kazuyuki Sugahara [c], Luisa Roncali [a], Roberto Perris [b, d, *]

[a] Department of Human Anatomy and Histology, University of Bari School of Medicine, BARI, Italy
[b] Division for Experimental Oncology 2, The National Cancer Institute Aviano, CRO-IRCCS, AVIANO (PN), Italy
[c] Frontier Research Center for Post-Genomic Science and Technology, Faculty of Advanced Life Science, Graduate School of Life Science, Hokkaido University, Kita-ku, Sapporo, Japan
[d] Department of Genetics, Microbiology and Anthropology, University of Parma, PARMA, Italy

Received: September 22, 2008; Accepted: January 23, 2009

Abstract

Aggrecan is a component of the CNS extracellular matrix (ECM) and we show here that the three primary alternative spliced transcripts of the aggrecan gene found in cartilage are also present in the adult CNS. Using a unique panel of core protein-directed antibodies against human aggrecan we further show that different aggrecan isoforms are deposited in perineuronal nets (PNNs) and neuropil ECM of Brodmann's area 6 of the human adult cerebral cortex. According to their distribution pattern, the identified cortical aggrecan isoforms were subdivided into five clusters spanning from cluster 1, comprised isoforms that appeared widespread throughout the cortex, to cluster 5, which was an aggrecan-free subset. Comparison of brain and cartilage tissues showed a different relative abundance of aggrecan isoforms, with cartilage-specific isoforms characterizing cluster 5, and PNN-associated isoforms lacking keratan sulphate chains. In the brain, isoforms of cluster 1 were disclosed in PNNs surrounding small-medium interneurons of layers II–V, small-medium pyramidal neurons of layers III and V and large interneurons of layer VI. Aggrecan PNNs enveloped both neuron bodies and neuronal processes, encompassing pre-terminal nerve fibres, synaptic boutons and terminal processes of glial cells and aggrecan was also observed in continuous 'coats' associated with satellite, neuron-associated cells of a putative glial nature. Immunolabelling for calcium-binding proteins and glutamate demonstrated that aggrecan PNNs were linked to defined subsets of cortical interneurons and pyramidal cells. We suggest that in the human cerebral cortex, discrete, layer-specific PNNs are assembled through the participation of selected aggrecan isoforms that characterize defined subsets of cortical neurons.

Keywords: proteoglycans • aggrecan isoforms • perineuronal nets • brain extracellular matrix • human cerebral cortex

Introduction

Our first knowledge of the amorphous extracellular matrix (ECM) surrounding and interspacing neurons and glia of the CNS dates back to the late 19th century, thanks to the advent of techniques enabling more detailed histological investigations of the amorphous material assembled around neuronal cell bodies and processes, later denominated *pericellular nets* [1–3]. After decades of oblivion, new, progressive exploration of the molecular composition of the nervous tissue ECM identified structures that appeared densely scattered throughout the neuropil, concentrated around neuronal cell bodies and were baptized perineuronal nets (PNNs). The CNS ECM is now known to encompass tenascins, hyaluronan and proteoglycans (PGs) that, together with a number of other ECM components, form intricate networks [4–8]. Within these networks PGs were first discovered to be present in nervous tissues by Richard and Rene Margolis in the mid-1970s [9] and were subsequently demonstrated to be critical constituents of the developing and adult brain ECM [10–13]. Some members of the PG family appear rather nervous tissue-specific, such as brevican,

*Correspondence to: Prof. Roberto PERRIS,
Department of Genetics, Microbiology and Anthropology,
University of Parma, Via G.P. Usberti 11/A,
43100 Parma, Italy.
Tel.: +39-0521-906601
Fax: +39-0521-906019
E-mail: rperris@cro.it

doi:10.1111/j.1582-4934.2009.00694.x

neurocan, testican-1 and -2 and neuroglycan C, whereas others, such as syndecans and PG-M/versicans, are widely distributed in many tissues throughout the body [14]. An abundant presence of PGs in PNNs was originally demonstrated by combining differential enzymatic digestion, lectin-based histology, ultrastructural analyses and immunohistochemistry [15–25]. These combined approaches made it possible to gain information about the distribution and extension of PGs throughout the CNS, ascertain their association with neurons residing within different areas and disclose individual PGs and their molecular partners within PNNs. However, the precise PG composition of PNNs of the human brain, the reciprocal interactions that these constituents may engage in, their turnover, and their differential arrangement in relation to the distribution of distinct neuronal subtypes, have not yet been completely elucidated.

Lecticans are known to be the most prominent ECM PGs in PNNs, but with the exception of deletion of the versican gene (impossible to evaluate up to now due to early embryonic death), deletion of the other murine lectican genes has yielded equivocal phenotypes and the actual consequences of aggrecan removal on brain development remain a particularly intriguing issue [13, 26]. All members of the lectican family have been shown to be synthetic products of cultured multipotent neural progenitor cells [12, 27], capable of reproducing PNN-like structures [28], and aggrecan seems to be specifically involved in neural cell–cell aggregation phenomena [29–30]. Other investigations have highlighted that avian and rodent neurons may express aggrecan [26, 31–33]. Thus, although some information has accumulated regarding the putative expression of aggrecan in the adult CNS of higher vertebrates, little is known about the detailed distribution of this specific PG in human brain. In this study, we have approached the problem by utilizing a unique panel of partially characterized monoclonal antibodies recognizing distinct aggrecan isoforms.

Materials and methods

Production and specificity of anti-aggrecan antibodies

Balb/c females were immunized with purified human articular cartilage aggrecan (kindly provided by Dr. Dick Heinegård, Department of Cell and Molecular Biology, University of Lund, Sweden) according to standard protocols involving repeated intraperitoneal and intravenous injection of the immunogen dissolved in complete Freund's adjuvant. This immunization protocol did not evoke any apparent pathological condition in the mice, such as the osteoarthritis or rheumatoid arthritis-like conditions previously reported with different immunization regimes and/or aggrecan variants. Spleen cells were fused with NS1 myeloma cells and the resulting hybridoma cells were screened by ELISA against intact and chondroitinase ABC/endo-β-galactosidase-digested aggrecan (see below). All identified reactive original hybridoma oligoclones (>25) reacted equally well with intact and enzyme-digested PG. Among these clones, 18 were selected and eventually subcloned to obtain stable monoclonal hybridomas coded: 4F8, 8E10, 7E1, 6F4, 6E5, 8G4, 2G5, 5B11, 4F4, 5C5, 5D3, 5G2, 5F12, 5G5, 3C7, 7B7, 7C9 and 7D4. Antibody classes were determined with the Ig-determination kit (Bio-Rad, Hercules, CA, USA) and all monoclonal antibodies were found to be IgG_1 and IgG_{2a}, except for clone 7E1 that was found to be an IgM. Control antibodies 3B3 (anti-chondroitin-6-sulphate stub; MO225 and 2C6, anti-native chondroitin-4-sulphate; 1B5, anti-unsulphated chondroitin stub; were obtained from Sigma Aldrich (St. Louis, MO, USA) and Seikagaku Corporation (Tokyo, Japan).

Solid-phase immunoassay

Binding studies with immobilized antigens were performed according to a minor modification of previously detailed assays [34]. Purified aggrecan was treated either chemically or with different enzymes in solution and then immobilized on plastic, nitrocellulose or PDVF membranes, or directly coated in the native form onto these solid supports. For the majority of the solid-phase immunoassays, coating was performed with overnight incubation at 4°C on 96-well plates (Nunc Maxisorp™, Thermo Fisher Scientific, Rochester, NY, USA) with 0.3 μg/well aggrecan (based on the entire mass of the PG, *i.e.* core protein plus glycosaminoglycan/carbohydrate moieties) dissolved in 0.1 M bicarbonate buffer, pH 9.2, followed by blocking with 1% bovine serum albumin (BSA) in the same buffer. PG-coated wells were either incubated directly with the primary antibodies or firstly digested for 1 hr at 37°C with the following carbohydrate/glycosaminoglycan-directed enzymes (obtained from Roche, [Segrate, Italy] Seikagaku Corporation, ICN Biochemicals [Aurora, OH, USA] and Sigma) at the given concentrations: keratanase I (0.01 U/ml in 50 mM Tris-HCl buffer, pH 7.6), chondroitinase ABC and ACII (0.01 U/ml in 50 mM Tris-HCl buffer, pH 7.6), keratanase II (0.01 U/ml in Na-acetate buffer, pH 6.5), endo-β-galactosidase (0.01 U/ml in 50 mM Na-acetate buffer, pH 5.8), *Streptomyces* hyaluronidase (0.15 U/ml, 50 mM Tris-HCl buffer, pH 7.6), β-galactosidase (0.01 U/ml in 100 mM Na-citrate buffer with 10% glycerol, pH 4.3), neuraminidases from *Clostridium perfringens* (0.2 U/ml in Na-acetate buffer, pH 5.5, 5.0 and 5.8, respectively), *N*-glycosidase F (0.01 U/ml 50 mM Na-citrate buffer with 10% glycerol, pH 5.0), *N*-acetyl-β-D-glucosaminidase (1:10,000 dilution in 50 mM Na-acetate, pH 5.0), endoglycosidases H and F (0.01 U/ml in 50 mM Na-sodium acetate buffer, pH 5.8). In other cases, immobilized PGs were digested with trypsin (5 μg enzyme/500 μg PG), 0.5 M LiOH at 4°C overnight (with and without prior digestion with chondroitinase ABC or ACII), periodate at 4°C overnight, or chemically desulphated by treatment with 50 mM HCl in 100% methanol for 4 hrs at room temperature (RT) or mildly β-eliminated by treatment with 1 M periodate, 1 M $NaBH_4$ or alkaline phosphatase for 1–3 hrs at RT, followed by extensive washing with PBS. Microwells were also coated with a number of control PGs and PG fragments which included: a recombinant fragment corresponding to a segment of human aggrecan encompassing the G1-IGD-G2 regions (R&D Systems, Inc., Minneapolis, MN, USA); bovine cartilage decorin (Sigma), bovine cartilage biglycan (Sigma), human fibromodulin (kindly provided by Dick Heinegård), bovine nasal cartilage aggrecan (kindly provided by Dick Heinegård), chick epiphysial cartilage aggrecan, EHS mouse tumour perlecan (Sigma), PG-M/versicans purified from bovine aorta as previously described [35], PG-M/versicans isolated from human follicular fluid and kindly donated by Anders Malmstrom (University of Lund, Sweden), a mixture of keratocan–mimecan–lumican purified from bovine aorta (kindly provided by James Funderburgh, McGowan Institute for Regenerative Medicine, Pittsburg, PA, USA), or recombinant eukaryotic fragments corresponding to the lectin-like domain of aggrecan (kindly given by Anders Aspberg, University of Lund, Sweden). Coatings with the PGs were routinely followed by blocking with 1% BSA in bicarbonate buffer for 1 hr at RT, extensive washings and incubation for 1 hr at RT with the antibodies diluted 1:1 to 1:200 for supernatants and ascites

fluids, and 1 μg/ml of purified IgGs. Excess unbound antibody was washed away and detection of the bound antibody was accomplished by a further 1 hr of incubation of the plates with HRP-conjugated goat antimouse secondary antibodies (Invitrogen-Zymed, Carlsbad, CA, USA) diluted 1:1000 in PBS with 1% BSA and colorimetric detection of the peroxidase with 2,2′-azino-di[3-ethyl-benzthiazolinsulfonate].

SDS-PAGE and immunoblotting

Intact and enzyme-digested human cartilage aggrecan and brain tissue homogenates were resolved by either SDS-PAGE (3–8% gradient gels) or agarose gel electrophoresis (1.2% gels; [35]) in the presence of SDS and under reducing and non-reducing conditions. Resolved polypeptides were electro-transferred onto nitrocellulose membranes, which were subsequently saturated with 4% α-casein (Sigma) dissolved PBS for 2–4 hrs at RT, followed by overnight incubation at 4°C with primary antibodies diluted as described for solid-phase binding assays in PBS containing 1% α-casein. After extensive washings, membranes were further incubated with HRP-conjugated goat antimouse secondary antibodies diluted 1:1000 in the same buffer for 1 hr at RT, followed by chemiluminescent antibody detection with the ECL Plus kit using the appropriate HyperFilm ECL membranes (Amersham-Pharmacia, Uppsala, Sweden).

RNA extraction and RT-PCR

Total RNA from different regions of the human foetal and adult brain was obtained from Cell Application, Inc. (San Diego, CA, USA). RNA isolated from adult articular cartilage was kindly provided by Dr. Paul Di Cesare (University of California Davis, USA). 5 μg of each of these RNAs were treated with the DNAsi Free kit (Ambion, Austin, TX, USA) and 1 μg was retro-transcribed with the SuperScriptTM III First-Strand Synthesis SuperMix according to the manufacturer's instructions. cDNAs were probed with the HPRT gene, using the following primers, forward, *5-gcttgctggtgaaaaggac-3′*; and reverse *5′-gtcaagggcatatcctacaac-3′*, for intactness and appropriateness for RT-PCR analyses and subsequently examined for the presence of aggrecan transcripts with the following primer sets: aggrecan gene (ACAN)627, *5′-gggtcaacagtgcctatcag-3′*; ACAN839, *5′-gggtgtagcgtgtagagatg-3′*; ACAN6773 *5′-gactcacacagtcgaaacag-3′*; ACAN7021, *5′-ggaagtggcggtaacagt-3′*; using the following conditions: $MgCl_2$ 1.4 mM, Primer 0.75 μM, dNTPs 0.3 mM, GoTaq (Promega, Madison, WI, USA) 0.05U and initial denaturing of the cDNA (5 min. at 95°C) with 32 cycles of 95°C for 30 sec., 56°C for 30 sec. and 72°C for 30 sec. To discriminate between the aggrecan C and E isoforms, a new amplification with primer ACAN forward-2, and the primer ACAN reverse-3, *agctccgcttctgtagtct* was carried out.

Immunohistochemistry

Six-layered cerebral cortex samples from the lateral premotor area of the left frontal lobe, Brodmann's area 6, were collected during autopsy (within 24 hrs) of eight persons with no signs of neurological disease (Table S1). Cortical samples (≤0.5 cm thick) were dissected and fixed by immersion in an acetic acid-free Bouin's solution for 4 hrs at 4°C and then washed in PBS. Half of the samples were embedded in paraffin and cut into 5-μm serial coronal sections collected on Vectabond™ treated slides (Vector Laboratories, Inc., Burlingame, CA, USA). Initially, sample comparability, tissue structure preservation and integrity of PNNs were morphologically ascertained on routinely haematoxylin and eosin stained sections and on sections labelled with the lectin *Wisteria floribunda agglutinin* (WFA) or with antibodies to tenascin-C and -R. Each of the eight examined brains showed similar tissue structure preservation and immunoreactivity patterns. For WFA labelling, sections were rehydrated in lectin buffer (LB; Tris-HCl, 1.45 M NaCl, 0.01 M $MgCl_2$ and 0.01 M $CaCl_2$; pH 7.6), treated with 1% H_2O_2 in 90% methanol for 20 min. at RT to quench endogenous peroxidase activity, washed twice in LB and incubated for 30 min. at 37°C with biotinylated WFA (diluted 1:100 in LB; Vector Laboratories, Inc.). Labelled sections were then washed, sequentially incubated with HRP-streptavidin (Vector Laboratories, Inc.) and the substrate-chromogen 3-amino-9-ethylcarbazole (AEC, Vector Laboratories, Inc.) and counterstained with haematoxylin prior to coverslipping with Glycergel mounting medium (Dako Corporation, Carpinterla, CA, USA). For immunolabelling for tenascin-C and -R, sections rehydrated and quenched as described above were processed for heat- and enzyme-mediated antigen retrieval by microwave pre-treatment in 0.01 M citrate buffer (pH 6.0) for 15 min. at 750W and subsequent digestion with trypsin II (1 mg/ml with $CaCl_2$ in PBS; Sigma-Aldrich, St. Louis, MO, USA) for 1 min. at 37°C. Sections were then sequentially incubated with blocking buffer (BB; PBS, 1% BSA, 2% FCS; Dako Corporation) for 30 min. at RT, one of the three primary antibodies, mouse anti-tenascin C (diluted 1:60 in BB; Novocastra, Newcastle, UK), rabbit anti-tenascin C and goat anti-tenascin R (both diluted 1:50 in BB; Santa Cruz Biotechnology, Santa Cruz, CA, USA) overnight at 4°C, appropriate species-specific biotinylated secondary antibodies (diluted 1:150 in BB; Vector Laboratories, Inc.), HRP-streptavidin (1 μg/ml; Vector Laboratories, Inc.) and AEC substrate (Vector Laboratories, Inc.). Sections were finally counterstained with haematoxylin and coverslipped by Glycergel (Dako Corporation). Negative control sections were prepared by omitting the primary antibodies and pre-adsorbing the primary antibodies with an excess of antigen where available. Reference immunolabellings for aggrecan and tenascins were performed on human laryngeal cartilage and glioblastoma multiforme specimens [36], respectively. Two specimens of human laryngeal cartilage were collected at autopsy, fixed, sectioned and immunolabelled in the same way as cerebral cortical sections. Reference glioblastoma specimens were collected from three patients who underwent surgical resection of the tumour at the Department of Neurosurgery, University Hospital Zurich. The WHO grade was confirmed by the Institute of Neuropathology, University Hospital of Zurich. Sampling and handling of human cerebral cortex and laryngeal specimens conformed to the ethical rules of the Department of Pathology, Medical School, University of Bari, Italy, and formal approval for manipulation of these specimens was obtained from the local Ethics Committee in compliance with the principles stated in the Declaration of Helsinki. All manipulations of glioblastoma specimens were conducted in accordance with the Declaration of Helsinki and approved by the Ethics Committee of the Canton Zurich. Informed written consent was obtained from all the surgical patients. For immunolabelling with anti-aggrecan antibodies, adjacent paraffin sections of the cerebral cortex were stained according to the HRP-streptavidin method described above, with each of the 18 anti-aggrecan antibodies used in this study – 4F8, 8E10, 7E1, 6F4, 6E5, 8G4, 2G5, 5B11, 4F4, 5C5, 5D3, 5G2, 5F12, 5G5, 3C7, 7B7, 7C9 and 7D4 (diluted 1:10 in BB) – and with a panel of 9 reference anti-aggrecan antibodies produced by R&D Systems, Inc. and provided for this study within the framework of an ongoing cooperation. Initial screening of these antibodies showed that only 3 of them recognized aggrecan isoforms of the cerebral cortex, whereas a fourth clone reacted with aggrecan of cartilage (Table S2). However, only clone 179509 was found to yield a satisfactory reactivity on paraffin-embedded specimens and was therefore used throughout this study as a reference anti-aggrecan antibody (r-aggrecan). Cortex sections were also stained with

anti-keratan sulphate antibody 373E1 [34]. The staining procedures on our 18 anti-aggrecan antibodies were carried out with and without prior enzymatic digestion with either chondroitinase ABC (0.6 U/ml diluted in Tris-HCl pH 7.6; Sigma-Aldrich) or keratanase-I or -II (Sigma-Aldrich and Seikagaku Corporation). Negative controls were prepared by omitting the primary antibodies and pre-adsorbing the primary antibodies with an excess of antigen.

Confocal laser microscopy

Parts of the collected specimens were sectioned at 20-μm thickness using a vibrating microtome (Leica; Milton Keynes, UK) and the sections were collected in PBS at 4°C as free-floating. Single and double immunolabellings were performed on free-floating sections as described below. Following staining the sections were examined under the Leica TCS SP2 confocal laser scanning microscope (Leica Microsystems, Mannheim, Germany) using a sequential scan procedure during image acquisition of double-labelled sections. Confocal images were taken at 250–500-nm intervals through the *z*-axis of the sections. Images from individual optical planes and image projections of stacks of serial optical planes were analysed by Leica confocal software (Multicolor Package; Leica Microsystems). The mouse IgG_1 anti-aggrecan antibody 5D3 (diluted 1:10 in BB) was revealed either singly, in combination with biotinylated WFA (diluted 1:100 in LB; Vector Laboratories, Inc.), used as a reference marker for PNNs, or in combination with reference aggrecan (R&D Systems, Inc., clone 179509, IgG_{2b}; 1:20 dilution in BB). Sections were sequentially incubated with 0.5% Triton X-100 in PBS for 30 min. at RT, BB for 30 min. at RT, and antibody 5D3 (single immunolabellings), or a mixture of 5D3 and one of the above antisera (for double immunolabellings), overnight at 4°C. Single-labelled sections were incubated with biotinylated horse antimouse IgG (diluted 1:200 in BB; Vector Laboratories, Inc.) for 1 hr at RT and with fluorescein-avidin D (diluted 1:125 in BB; Vector Laboratories, Inc.). In double immunolabellings with mAb 5D3 and biotinylated WFA or the reference anti-aggrecan antibody, antibody binding was revealed using either Alexa 488-conjugated goat antimouse IgG_1 or a rabbit antimouse IgG_{2b} Alexa 555-conjugated secondary antibody (diluted 1:200 in BB; Invitrogen), whereas WFA binding was detected with Texas red-conjugated avidin D (1:125 dilution; Vector Laboratories, Inc.). In order to reveal the association between PNNs and the main populations of cortex neurons, antibody 5D3 was utilized in double immunolabellings with one of the polyclonal antisera against the calcium binding proteins (Ca^{2+}BPs), rabbit anti-calbindin D-28k, rabbit anti-calretinin, or goat anti-parvalbumin adopted as markers for cortex interneurons, used at 1:2000, 1:1000 and 1:1000 dilution, respectively (Swant, Bellinzona, Switzerland), or with a rabbit polyclonal antiserum against the neurotransmitter glutamate (Glu) (diluted 1:25 in BB; Chemicon, Temecula, CA, USA), known to be a recognized marker for most of the cortical pyramidal neurons. In these double immunolabelling experiments, antibody 5D3 was revealed with a biotinylated horse antimouse secondary antibody and the fluorescein-avidin D complex (Vector Laboratories, Inc.) and the other alternatively combined primary antibodies were detected with the appropriate Alexa 555-conjugated secondary antibodies (diluted 1:200 in BB; Invitrogen). To determine the relationships between aggrecan PNNs and the perineuronal nerve and glial terminals, the same protocol described above was utilized to perform double immunostainings with antibody 5D3 in combination with either a rabbit polyclonal antibody against the astroglial marker glial fibrillary acidic protein (GFAP; pre-diluted antiserum re-diluted 1:2 in BB; ImmunoStar, Hudson, WI, USA) or with a rabbit polyclonal antiserum against synaptophysin, as a marker for nerve terminals (diluted 1:20 in BB; Novocastra).

Morphometry

A semi-quantitative evaluation of the aggrecan isoform distribution was carried out on both laryngeal and brain paraffin sections using the image analysis system VIDAS 2.5 (Kontron Elektronik GmbH, Eching, Germany) supported by a high-resolution video camera (SPOT Insight Colour, Diagnostic Instruments, Sterling Heights, MI, USA). Multiple fields, obtained from three sections labelled with each of the anti-aggrecan antibodies assayed in parallel on cartilage and brain tissues, were acquired at 20× (field total area measuring 75,440 μm^2). The images were digitalized, optimized by contrast enhancement functions and by digital filters, and segmented by an interactive threshold-definition modality capable of discriminating aggrecan-positive PNNs on neuronal bodies and processes and aggrecan reactivity in cartilage ECM. The resulting binary image was processed by measurement functions to obtain the percentage of aggrecan immunoreactive areas. The results for the laryngeal cartilage were expressed according to the following percentage ranges of immunoreactive area: 1–25 = +; 26–50 = ++; 51–75 = +++ and 76–100 = ++++. For the cerebral cortex, the PNNs immunoreactivity area was expressed according to the following estimated percentage ranges: 1×10^{-5} to 1×10^{-3} = +; 2×10^{-3} to 0.20 = ++; 0.21–0.40 = +++ and 0.41–1 = ++++. According to these ranges of aggrecan distribution, different clusters (clusters 1–4) of aggrecan isoforms recognized by sets of antibodies were identified in the cerebral cortex and Bonferroni's multiple comparison test was applied to define statistical significance. Microphotographs of cerebral cortex processed for morphometric analyses were also used for the immuno-localization of aggrecan PNNs in the cortical layers. Antibodies representative of the identified clusters, cluster-1 (5D3), -2 (7C9), -3 (5G5) and -4 (2G5) were utilized for the immunostaining of three sets of cortex serial sections and for each set the sections were alternatively labelled according to the following sequence: cluster-1, -2, -1, -3, -1, -4 and -1. The section area (9 mm^2) was then digitalized at 20× for a total of 120 microscopic fields (field total area measuring 75,440 μm^2), these were then compared to verify the presence of PNNs stained by different isoforms in adjacent sections. A quantitative evaluation of the differently labelled neuronal populations and/or of their association with aggrecan 5D3-PNNs was performed on vibratome sections double-stained by immunofluorescence and analysed by confocal microscopy. Neurons double-stained with 5D3/WFA, 5D3/r-aggrecan, 5D3/Ca^{2+}BPs, 5D3/calbindin, 5D3/calretinin, 5D3/parvalbumin and 5D3/Glu, were counted by computer-aided morphometry applied on confocal projection images according to an interactive morphometric procedure. The fluorescence signal was singly recorded on both red and green channels as multiple fields obtained from six randomly chosen sections. Each field was acquired at 20× and after fluorescence enhancement and binary conversion, the resulting binary image was segmented by an interactive threshold-definition modality using the image analysis system VIDAS 2.5 (Kontron Elektronik) and processed by measurement functions. The labelled neurons were detected and the results were expressed as the percentage of marked neurons per total section area (mean value ± S.D.).

Results

Specificity of anti-aggrecan antibodies and putative nature of the recognized epitopes

A unique panel of anti-human aggrecan antibodies was produced using a native A1D1 aggrecan preparation from adult human

Table 1 Characteristics of anti-aggrecan antibodies*

Antibody code	Epitope location	Trypsin sensitivity†	Species cross-reactivity††
4F8	G1-IGD-G2§	125–165, ~320 kD	+++
8E10	GAG-Linkage region¶	~320 kD	+
7E1	Lectin-like module of G3 domain$	205 kD	++
6F4	–	55, 65, 95 kD	+++
2G5	Conformational**	+	–
5B11	Conformational	85 kD	–
4F4	Conformational/G1-IGD-G2	+	++
5C5	G1-IGD-G2	+	++
5D3	–	+	–
5G2	Lectin-like module of G3 domain	320–420 kD	–
5F12	–	+	+++
5G5	G1-IGD-G2/GAG linkage region	+	–
6E5	Conformational/G1-IGD-G2	n.d.	++
8G4	Conformational	n.d.	–
3C7	*O*-glycan attachment site?	+	+++
7B7	GAG linkage region	+	–
7C9	*O*-glycan attachment site?	+	+
7D4	G1-IGD-G2/GAG linkage region	+	+++

*Antibody reactivity was examined in parallel by combined solid-phase binding assays (ELISA and dot-blotting, following membrane immobilization of the antigen) and Western blotting.

†Trypsin-digested aggrecan, deprived of its chondroitin and keratan sulphate chains, was immunoblotted following SDS-PAGE under both reducing and non-reducing conditions and the cumulative data are reported; '+' indicates that immunoreactivity was completely eliminated following digestion, whereas M_rs corresponds to the sizes of the tryptic fragments recognized in Western blotting by the given antibodies.

††These antibodies were found to cross-react to a variable extent with bovine nasal cartilage and bovine sclera aggrecans, but not with rat chondrosarcoma, chick epiphysial, shark or whale aggrecans; cross-reactivity levels were determined by solid-phase binding assays using human aggrecan as reference and are arbitrarily scored as follows: '–', no cross-reactivity; '+', 25–50%; '++', 50–75%; '+++' and 75–100% cross-reactivity.

§These antibodies were found to react in solid-phase binding assays with a recombinant eukaryotic fragment corresponding to an *N*-terminal fragment encompassing the G1 and G2 globules interspaced by the inter-globular domain-1 (G1-IGD-G2).

¶These antibodies were found to react in solid-phase binding assays with a recombinant eukaryotic fragment corresponding to the *C*-terminal lectin-like module of the G3 globular domain.

$The putative conformational nature of the epitopes was deduced by solid-phase binding assays and Western blotting involving prior reduction and alkylation (DTT/iodoacetamide) of chondroitinase-endo-β-galactosidase-digested aggrecan preparations.

**The epitope recognized by these antibodies is presumed to reside at the GAG core protein linkage region (GlcA-β 1–3Gal-β1–3Gal-β1–4Xyl-β1-*O*-Ser), as determined by solid-phase binding and competition assays using hexasaccharide peptides of this region.

articular cartilage of healthy donors that was enzymatically digested prior to use as immunogen in such a way as to eliminate its chondroitin and keratan sulphate chains. An immunization protocol was then adopted to avoid the commonly observed induction of arthritis-like conditions in the immunized animals. Due to the multidomain structure of aggrecan and the possibility that immunogenic epitopes could be represented by glycosylation moieties shared by other PG and non-PG molecules, specificity of the obtained hybridoma clones was ascertained using a number of purified PGs and ECM glycoproteins (see section 'Materials and methods'). Cross-species reactivity was further determined using aggrecans from bovine nasal cartilage, bovine sclera, rat

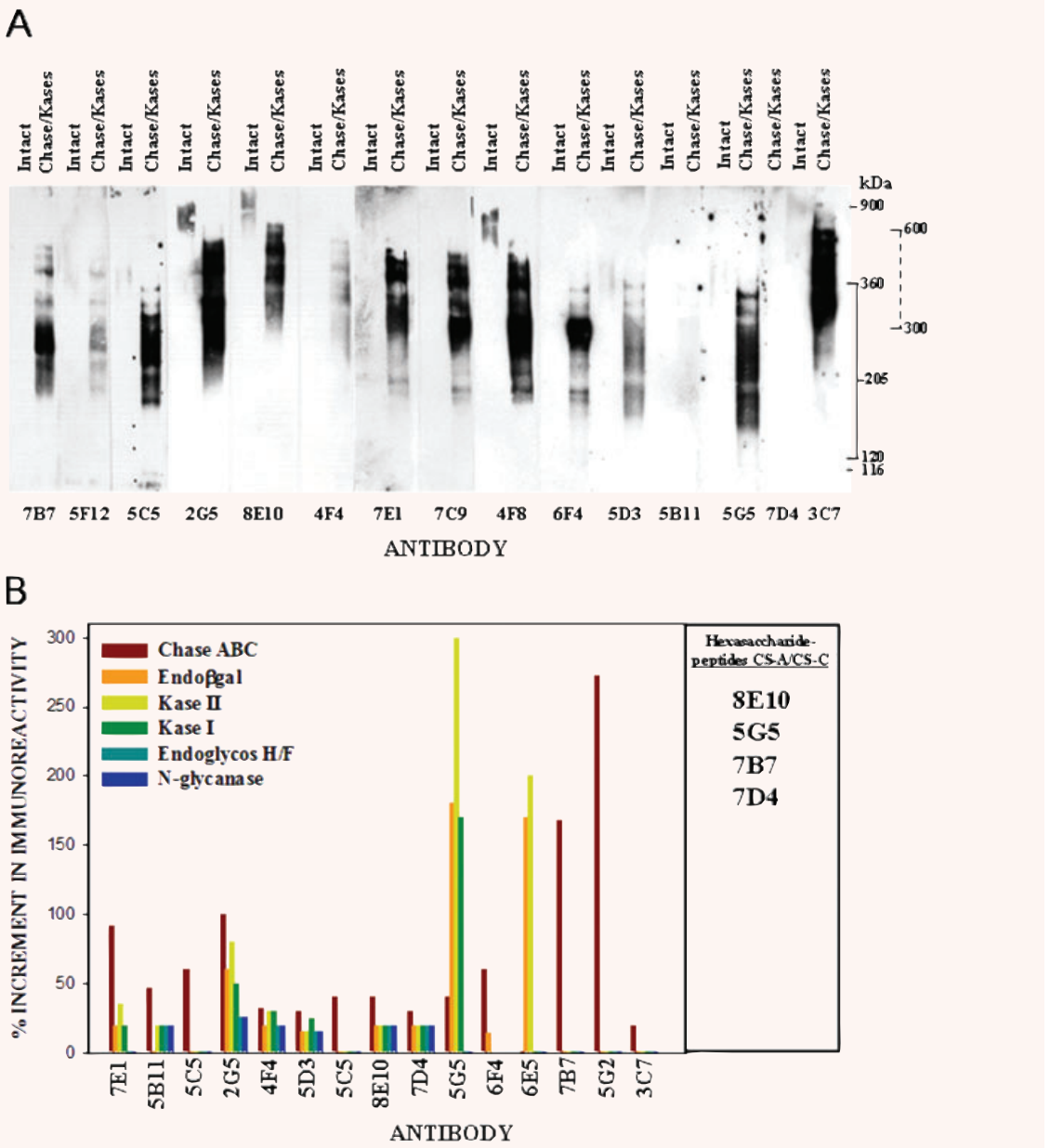

Fig. 1 (**A**) Immunoblotting pattern observed with the panel of anti-aggrecan antibodies and highlighting the structural diversity of aggrecan variants revealed by the antibodies in aggrecan preparations from human adult articular cartilage. Aggrecan variants purified from healthy cartilage were sequentially digested with chondroitinase ABC, endo-β-galactosidase and keratanase I, resolved by SDS-PAGE on 3–8% gradient gels under non-reducing conditions, blotted onto nitrocellulose and detected with the indicated antibodies. M_{rs} ranges reported on the right correspond to those previously identified by biochemical means in cartilage and including naturally occurring proteolytic fragments of the fully glycanated forms of the PG. A 900 kD M_r indication was extrapolated from the relative M_{rs} of bovine thyroglobulin and the unreduced laminin-1-nidogen complex from EHS. (**B**) Relative levels of immunoreactivity of different antibodies determined by solid-phase binding assays involving immobilized human cartilage aggrecan that was digested *in situ* or not with the indicated enzymes: Chase ABC, chondroitinase ABC; endo-β-gal, endo-β-galactosidase; Kase I and II, keratanase I and II; and endoglycosidase H/F. Data are reported as percentage reactivity increase when compared to undigested aggrecan. Increases above 21% were deemed significant, $P < 0.01$, 95% confidence interval. Similarly to antibody 3C7, antibodies 7C9, 5F12 and 4F8 showed no variation in reactivity.

chondrosarcoma, chick epiphysial cartilage and shark cartilage (Table 1). Immunoblotting of the immunogen after sequential digestion with chondroitinase ABC, keratanase I and keratanase II highlighted the variable banding, reflecting the aggrecan isoform patterning (Fig. 1A) associated with the multiform nature of the aggrecan variants generated by alternative splicing [37–39] and different proteolytic cleavages of the PG [40].

In addition to variations in the size and glycosylation patterns of the aggrecan core protein isoforms, the fact that even extensive digestion with chondroitinases and keratanases did not affect the numerous *N*- and *O*-linked glycan moieties had to be accounted for by the diversified molecular size pattern. In accordance with previous studies, the isoform core banding was in the range of 120–360 kD [40], with the predominant isoforms having a 240–260 kD core protein, whereas two lower mobility bands of more glycosylated aggrecan variants were disclosed at about 400 and 600 kD (Fig. 1A). Antibodies 5G2, 8E10 and 4F8, that were found to recognize the C-terminal portion of the molecule, also detected proteolytic fragments of aggrecan that weakly entered the 3% gel in the undigested form and had a M_r ~900–1000 kD (Fig. 1A).

Immunoreactive traits of the antibodies were further determined by immunochemical assays involving differential enzyme digestions combined with chemical treatments for partial or complete removal of glycan moieties. Antibody reactivity was found to be entirely unaffected by digestions with endo- and exo-glycosidases, fucosidases, neuraminidases and hyaluronidases (not shown), but was differentially affected by digestions with chondroitinase ABC, keratanase I and II and endo-β-galactosidase (Fig. 1B). The immunoreactivity of antibodies 6F4, 4F4, 5F12, 6E5, 7B7 and 7C9 was specifically augmented by preferential removal of keratan sulphate glycan chains with endo-β-galactosidase or keratanase II, indicating that the epitopes for these antibodies resided within or in the proximity of the keratan sulphate attachment domain of the PG.

Three of the antibodies were found to recognize a recombinant fragment corresponding to the lectin-like *C*-terminal domain of aggrecan (Table 1), suggesting that their epitopes may reside within the G3 globule of the PG. Several of the antibodies were likely to recognize conformational epitopes, *i.e.* sensitive to perturbation of the secondary or tertiary structure of the PG. Finally, clones 4F8, 4F4, 5C5, 5G5, 6E5 and 7D4 were found to recognize epitopes residing within the *N*-terminal G1-IGD-G2 region of aggrecan (Fig. 1A).

Since some of the antibodies showed enhanced immunoreactivity following removal of the glycosaminoglycan side chains we suggested that they could recognize epitopes in the proximity or within the linkage regions of these chains. To further analyse this possibility some of the antibodies were assayed against human and bovine cartilage aggrecans that had been extensively digested with chondroitinase ABC, followed by chondroitinase ACII and LiOH or periodate treatments. These additional tests confirmed that antibodies 3C7, 7D4, 8E10 and 5C5 potentially recognized an epitope nearby, or within the chondroitin sulphate-attachment region. To evaluate whether the phosphate group on the xylose residue of the linkage region was part of the epitope parts, we carried out competitive ELISA with alkaline phosphatase-treated PG, after exhaustive digestion with chondroitinase AC-II, as well as hexasaccharide peptides prepared from glycopeptides derived from whale and shark cartilage aggrecans. These experiments suggested that the epitopes of certain antibodies were in juxtaposition with the chondroitin sulphate-attachment sites and could comprise *O*-glycan moieties, or contain previously described uniquely sulphated galactose residues [41, 42]. In fact, antibodies 8E10, 5G5, 7B7 and 7D4 showed a weak reactivity to hexasaccharide peptides corresponding to the chondroitin-4-sulphate and -6-sulphate core protein linkage region of whale cartilage aggrecan (not shown).

Morphological and molecular verification of the integrity of post-mortem adult brain PNNs

The analysis of routinely haematoxylin and eosin stained sections of Brodmann's area 6 suggested satisfactory sample comparability and tissue preservation of specimens collected from deceased individuals with no histopathological signs of neurological disease (Table S1). Staining with lectin WFA showed the integrity of the PNNs in all the selected brains. In fact, in each of the analysed cerebral cortex samples the reference lectin revealed a similar staining pattern, characterized by a diffuse ECM immunoreactivity throughout all cortical layers and more concentrated in cortex layer III, and by well-defined PNNs associated with numerous cortical neurons from layer I to VI (Fig. S1A–E). Conversely, tenascins-C and -R, which are also established PNN components in developing and adult rodent brains, were found to be poorly expressed in the adult human cerebral cortex PNNs; some tenascin-C was restricted to the ECM of subcortical white matter, whereas tenascin-R was diffusely expressed in the cortical ECM but not in the PNNs (Fig. S2A, B, D). Unlike the situation in normal cortex, both tenascins were strongly expressed in the interstitial and perivascular compartments of glioblastoma lesions which were adopted as reference tissues (Fig. S2C, E).

Human brain expresses alternatively spliced forms of aggrecan

The ACAN maps on chromosome 15q26.1 and covers 71.92 kb containing 26 introns and 20 exons generating up to 15 different mRNA of which 10 are alternatively spliced and 5 are unspliced forms. The spliced mRNAs appear to differ due to differential truncations of the 3′ end, the presence or absence of four spliced exons, the presence of overlapping exons with different boundaries. The most abundant spliced isoforms previously described in cartilage and cartilage tumours are *isoforms B* and *C* (in the data bank an *isoform A* is also described but it is identical to the variant that has been denoted isoform *C*), while an additional isoform denoted *isoform F* has been described in breast stromal tissue. Finally, another alternative spliced form, *isoform E*, of the PG has

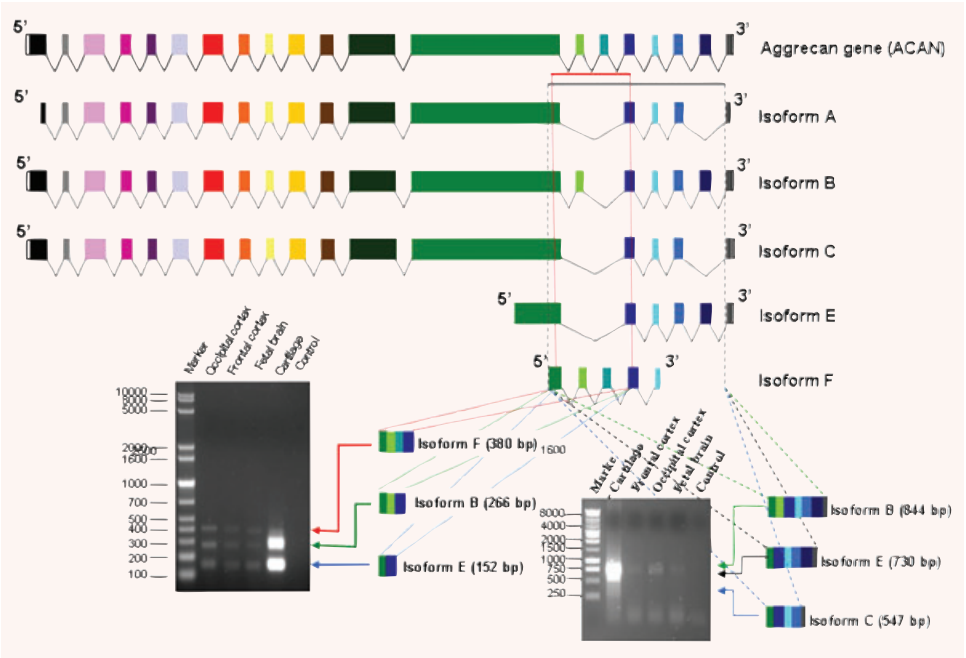

Fig. 2 Schematic diagram illustrating the primary structure of the human aggrecan gene (ACAN) and the prevalent alternative spliced transcripts previously identified in cartilage, mammary gland, brain, chondrosarcoma and glial tumours (*i.e. isoforms A*, *B*, *C*, *E* and *F*) and the expression pattern of these isoforms in different regions of adult and foetal human CNS. Adult articular cartilage tissue was used as reference.

been identified in human brain and oligodendroglioma. Other minor, more poorly defined isoforms that seem to arise through truncation of the 5′-end of the gene have been described in melanoma (*isoform G* and *H*), skin (*isoform G*), articular cartilage, colon, juvenile granulosa tumours and testis (*isoform D*). However, the possibility remains that these latter isoforms are mere fragments of *isoforms B* or *C*. We have therefore ignored these latter isoforms and have concentrated our analyses on the remaining isoforms, *isoforms B*, *C*, *E* and *F*, which we find to be present in all examined areas of the foetal and adult brain (Fig. 2).

Differential aggrecan isoform deposition in PNNs and cortical ECM

Aggrecan isoform expression in the cerebral cortex and reference cartilage ECM was evaluated in parallel by morphometry on adjacent tissue sections that were immunolabelled without prior enzymatic treatments and following either chondroitinase ABC or keratanase digestion. Semi-quantitative evaluation of aggrecan isoform distribution was carried out on both batches of sections and aggrecan isoform expression was scored from absent to abundant based upon the percentage of tissue area occupied by aggrecan-rich PNNs within the total field area analysed. Comparison of the staining patterns obtained prior to and after enzymatic predigestion of the sections indicated that, in the majority of cases, the intensity and extension of aggrecan isoforms did not change after chondroitinase digestion, with the exception of aggrecan isoforms recognized by antibodies 6E5 and 7B7, which became evident in layers II to VI after digestion, and in the case of isoforms revealed by antibodies 5C5 and 5B11, whose intensity levels appeared higher (Table 2). Neither quantitative nor qualitative changes in the overall distribution pattern of aggrecan isoforms were observed after keratanase pre-treatment of the sections.

Notably, the expression pattern of aggrecan isoforms in laryngeal cartilage was markedly different from that observed in the nervous tissue. For instance, antibodies 5G2 and 7B7 revealed isoforms that were highly expressed in cartilage, but hardly detectable in the cerebral cortex, while widespread cortical isoforms recognized by antibodies 5D3 and 4F4 were poorly expressed in cartilage (Table 2). Thus, aggrecan isoforms produced in the two tissues appeared to be entirely mismatched, with an essentially inverted distribution frequency of the different isoforms in the two tissues (Table 2). Immunoblotting on whole brain homogenates further confirmed the presence of diverse CNS aggrecan variants and highlighted both their divergent M_rs and complex glycanation patterns (Fig. 3C).

According to the distribution patterns in PNNs and neuropil ECM of the different cortical layers, aggrecan isoforms were clustered in five distinct groups denoted clusters 1 to 5 (Table 2; Figs. 3A, B and 4A–I). Aggrecan isoforms of cluster 1 included those recognized by antibodies 5D3, 7D4, 4F4, 5C5 and 6E5, and were found to be the most abundantly expressed in PNNs and ECM of layers II–VI. Isoforms of cluster 2, recognized by antibodies 7C9, 4F8 and 3C7, were similarly expressed in layers II–VI, albeit in a less widespread manner. Isoforms of cluster 3, identified by antibodies 5F12, 5G5, 5B11 and 7B7, were restricted to layers III–VI. Cluster 4 aggrecan isoforms, recognized by antibodies 5G2 and 2G5, were only detectable in solitary PNNs of neurons within cortical layer V and, finally, cluster 5 was comprised aggrecan isoforms recognized by antibodies 6F4 and 8E10, which were highly expressed in laryngeal cartilage and absent in brain (Table 2;

Table 2 Comparative patterns of aggrecan isoform distribution in PNNs of the human cerebral cortex and laryngeal cartilage

Antibody code	Laryngeal cartilage ECM*	Cerebral cortex PNNs†	Cerebral cortex ECM††	Cortical layer (PNNs)
Cluster 1				
5D3	+	++++	+++	II, III, IV, V, VI
7D4	+++	++++	++	II, III, IV, V, VI
4F4	++	++++	++	II, III, IV, V, VI
5C5§	+++	++++	++	II, III, IV, V, VI
6E5§	+++	++++	++	II, III, IV, V, VI
Cluster 2				
7C9	+	+++	++	II, III, IV, V, VI
4F8	+	+++	++	II, III, IV, V, VI
3C7	+	+++	+	III, V, VI
Cluster 3				
5F12	+	++	+	III, V, VI
5G5	–	++	+	III, V, VI
5B11§	+	++	+	III, V, VI
7B7§	++++	++	+	III, V, VI
Cluster 4				
5G2	++++	+▲	+	V
2G5	+	+▲	+	V
Cluster 5				
6F4	++	–	–	–
8E10	+++	–	–	–

*Laryngeal cartilage was used as a reference aggrecan-rich tissue to ascertain antibody reactivities and variations in aggrecan isoform distribution; the scoring adopted for the observed immunolabelling was in this case: '+', 1 – 25%; '++', 26 – 50%; '+++', 51 – 75%; '++++' and 76 – 100% of the tissue ECM immunolabelled.

†Immunoreactivity patterns of PNNs were morphometrically established as detailed in section 'Materials and methods' (+▲, indicates solitary aggrecan-containing PNNs) by threshold normalization of the immunolabelling signals detected above the diffuse signal of the neuropil aggrecan-containing ECM for each cortical layer and by adopting the following scoring with reference to the immunolabelled surface area: '+', 10^{-5}–10^{-3}; '++', 2×10^{-3}–0.20; '+++', 0.21–0.40 and '++++', 0.41–1.0 mm^2.

††Arbitrary levels of aggrecan isoform extension in the ECM of each cortical layer scored as: '–', not present; '+', scattered; '++', localized and '+++', widespread.

§Staining intensity and extension was enhanced by prior enzymatic digestion of the sections with chondroitinase ABC. Antibodies 7E1 and 8G4 did not detect any aggrecan isoforms in tissue sections under the immunostaining procedures adopted.

Figs. 3A, B and 4A–I). Complementary reference immunostaining for keratan sulphate moieties using antibody 373E1 [34], revealed that in human adult brain keratan sulphates were diffusely distributed through the ECM, but were largely absent in PNNs (Fig. 4J). While this finding suggests that PNN-associated aggrecan variants of human adult brain do not contain keratan sulphate and may also lack other keratan sulphate-bearing PGs, it does not preclude the possibility that human adult brain keratan sulphates may be prevalently associated with phosphocan as previously proposed.

To determine if aggrecan isoforms from the different clusters defined herein were present in the same PNNs recognized by antibodies detecting isoforms of cluster-1, serial cortical sections were alternatively immunostained with cluster-1 antibodies and with antibodies detecting aggrecan isoforms in each of the other

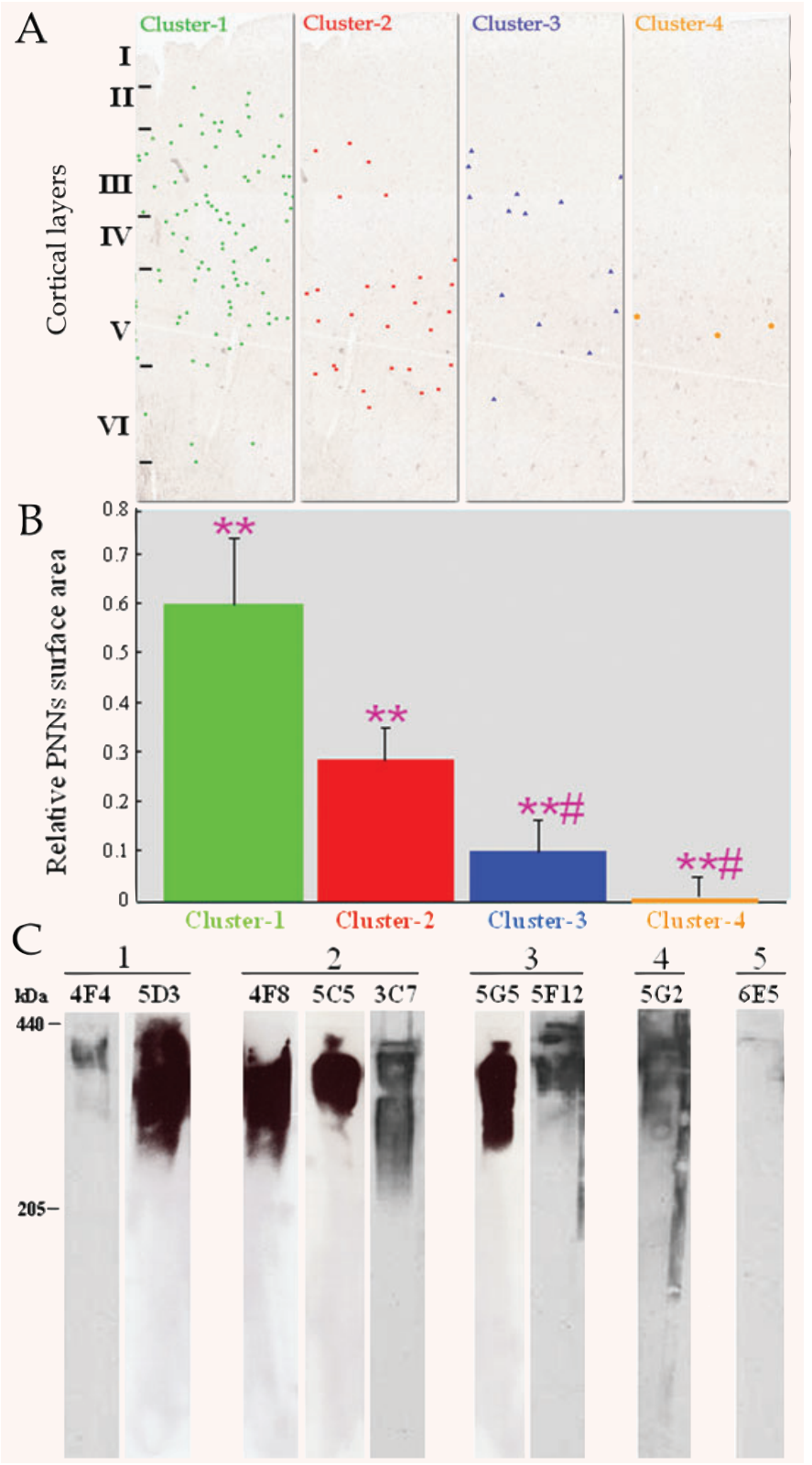

Fig. 3 (**A**) Topographical representation and (**B**) semi-quantitative evaluation of aggrecan isoform distribution in the different layers of Brodmann's area 6 in the human cerebral cortex (**, $P < 0.05$; #, $P < 0.01$). (**C**) Immunoblotting of whole brain homogenates with the indicated antibodies following sequential digestion of the lysate with chondroitinase ABC, endo-β-galactosidase and keratanase I, SDS-PAGE on 5–15% gradient gels under non-reducing conditions, and transfer onto nitrocellulose membranes.

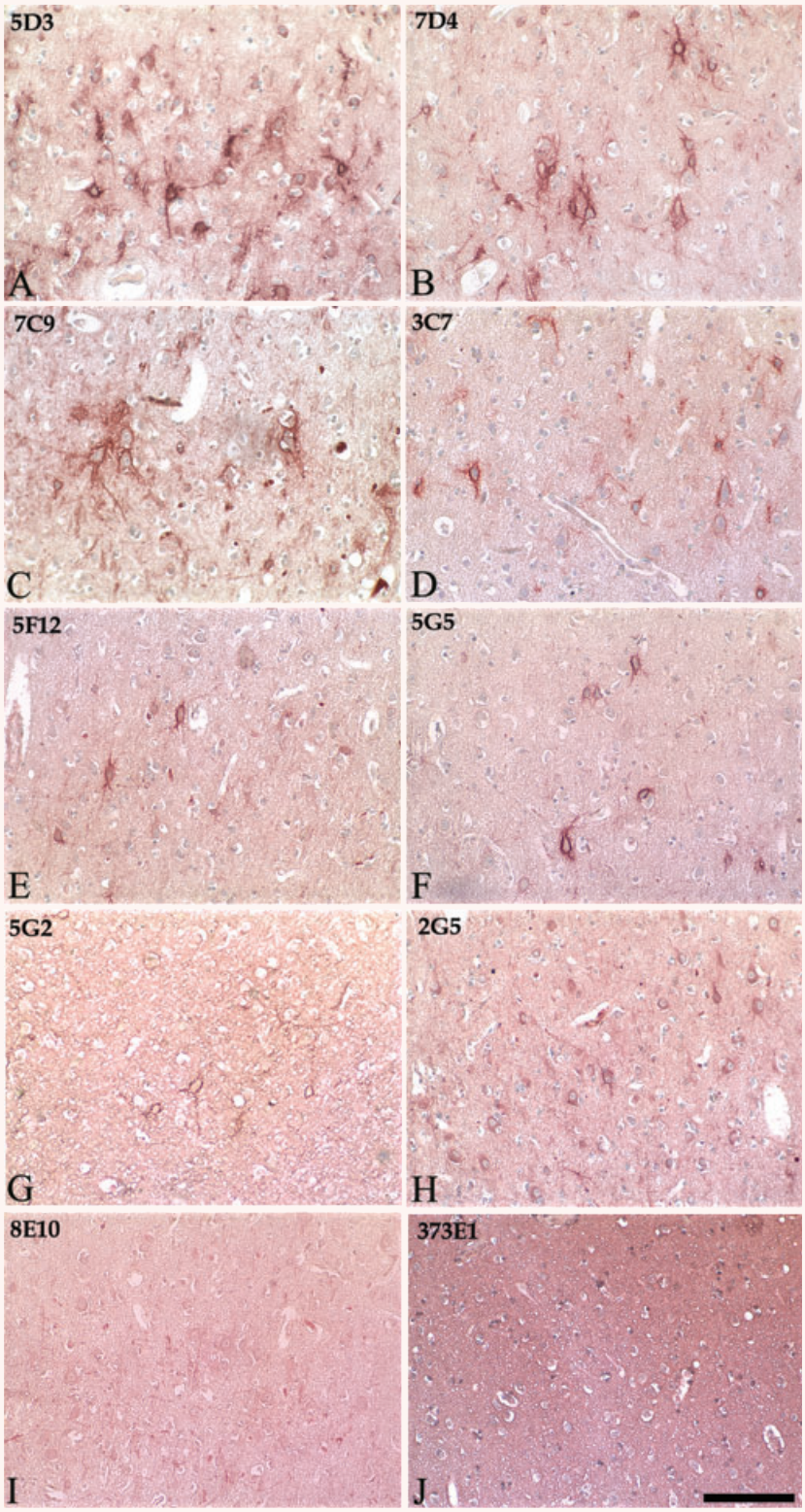

Fig. 4 (**A–I**) Overview of 9 aggrecan isoforms detected in the ECM and PNNs of cortical layer V of Brodmann's area 6, representative of the previously defined clusters: cluster 1, isoforms 5D3 and 7D4 (**A**, **B**), cluster 2, 7C9 and 3C7 (**C**, **D**), cluster 3, 5F12 and 5G5 (**E**, **F**), cluster 4, 5G2 and 2G5 (**G**, **H**), cluster 5, 8E10 (**I**). Keratan sulphate-bearing PGs are only detected in the neuropil ECM (**J**). Counterstaining with haematoxylin. Magnification bar: 100 μm.

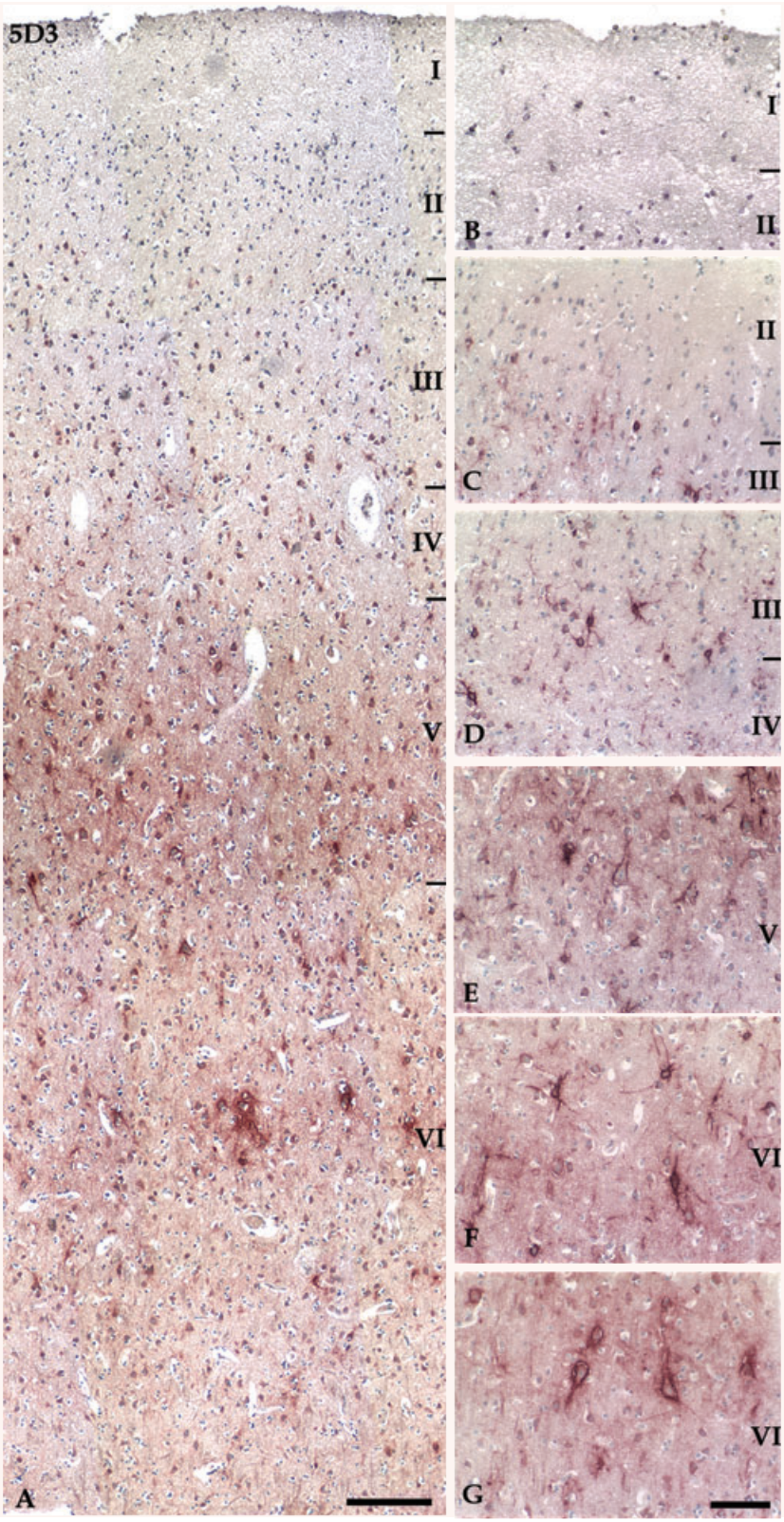

Fig. 5 Global view of aggrecan deposition in Brodmann's area 6 as determined by staining with antibody 5D3. No aggrecan deposition could be observed in the neuropil ECM of cortical layer I (**A**, **B**), whereas a progressively increased expression of the PG could be noted starting from the deeper regions of cortical layer II and spanning Brodmann's entire area up to cortical layer VI (**A**, **C–G**). Aggrecan-containing PNNs are observed in association with small-medium sized neurons of cortical layers III-VI (**A**, **C–G**) and larger neurons of cortical layers V and VI (**E–G**). High magnification views of the cortical layers containing aggrecan-rich PNNs show aggrecan deposits surrounding both the neuronal cell bodies and the extended processes (**C–G**). Counterstaining with haematoxylin. Magnification bars: (**A**) 400 μm; (**B–G**), 100 μm.

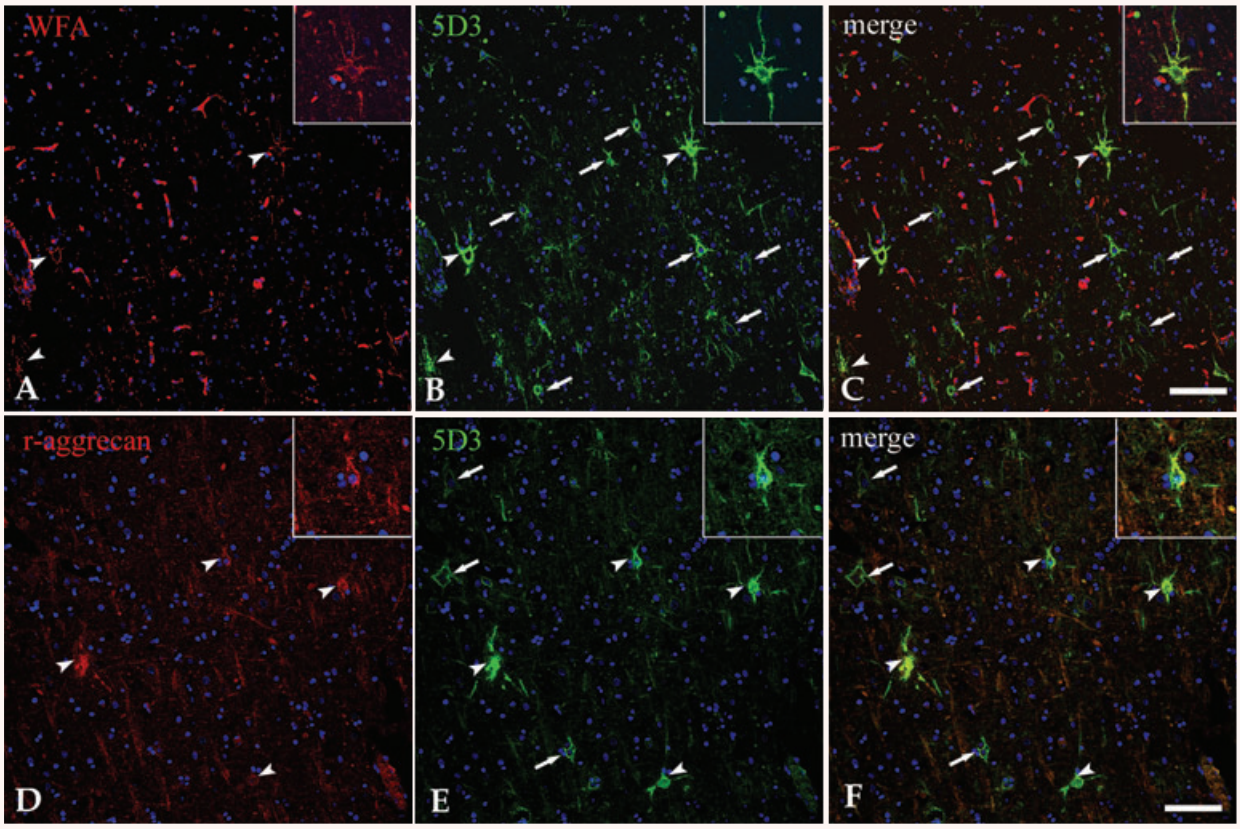

Fig. 6 Confocal laser microscopy images, representative of all the analysed brain samples, through Brodmann's area 6 double-labelled with lectin WFA and our anti-aggrecan antibody 5D3 (**A**–**C**), or with a combination of the antibody against reference aggrecan (r-aggrecan; clone 179509, R&D Systems, Inc.) and antibody 5D3 (**D**–**F**). Lectin WFA-stained PNNs are co-labelled by antibody 5D3 (arrowheads in **A**–**C**), (**B**) whereas other PNNs are labelled to different degrees only by antibody 5D3 (arrows, in **B** and **C**). Also note, at higher magnification, a double-stained polymorphous interneuron (*inset* in **A**–**C**) and the lectin WFA-stained cortical blood microvessels (**A**, **C**). (**D**–**F**) Reference aggrecan and our aggrecan 5D3 co-label a number of PNNs (arrowheads), whereas other PNNs are only stained by 5D3 (arrows in **E** and **F**). Counterstaining with the nuclear tracer TO-PRO-3. Magnification bars: 100 μm.

clusters. Isoforms of clusters-1 and -2 almost totally coincided in the same PNNs, although a larger number of PNNs had isoforms recognized by antibody 5D3 (Fig. S3A, B). A lower number of PNNs were revealed by antibodies from cluster-3 and all of these were also detected by cluster-1 antibodies (Fig. S3C, D). Finally, the few weakly reactive PNNs revealed by antibodies recognizing aggrecan isoforms of cluster 4 were always present also on sections stained by cluster-1 antibodies (Fig. S3E, F). These results demonstrated that aggrecan isoforms from clusters-2 to -4 contributed differently to the PNNs characterized by cluster-1 isoforms, which in turn showed the widest molecular variation.

The aggrecan isoform(s) recognized by antibody 5D3 and pertaining to cluster-1 was unique in that it was weakly expressed in laryngeal cartilage, but appeared abundant in brain (Table 2). We therefore investigated in more detail the distribution of this putative isoform(s). It was found to be virtually absent in both PNNs and ECM of cortical layer I (Fig. 5A and B) and widespread in PNNs and ECM of cortical layers II–VI. This aggrecan isoform distinctly revealed PNNs associated with numerous cortical interneurons and a restricted number of pyramidal cells. The ECM encompassing this isoform initiated at the boundary between cortical layers II and III and was progressively intensified in the deeper cortical layers, with a peak seen in cortical layer V (Fig. 5A, C–G). Aggrecan-containing PNNs were also revealed around a few smaller interneurons of cortical layer II (Fig. 5A and C) and more evidently around numerous small- to medium-sized polymorphous interneurons of cortical layers III. Within the same layer, although less evident, aggrecan enriched PNNs were also observed to be associated with small- to medium-sized pyramidal cells (Fig. 5A, C and D). In cortical layer IV, only smaller interneurons appeared to be sparsely decorated by aggrecan-containing PNNs (Fig. 5A and D), whereas within cortical layer V these PNNs were detected around numerous small- to medium-sized sized polymorphous interneurons and a few medium-sized pyramidal neurons (Fig. 5A and E). Finally, at the level of cortical layer VI, conspicuous aggrecan-containing PNNs were associated with sparse, medium-sized

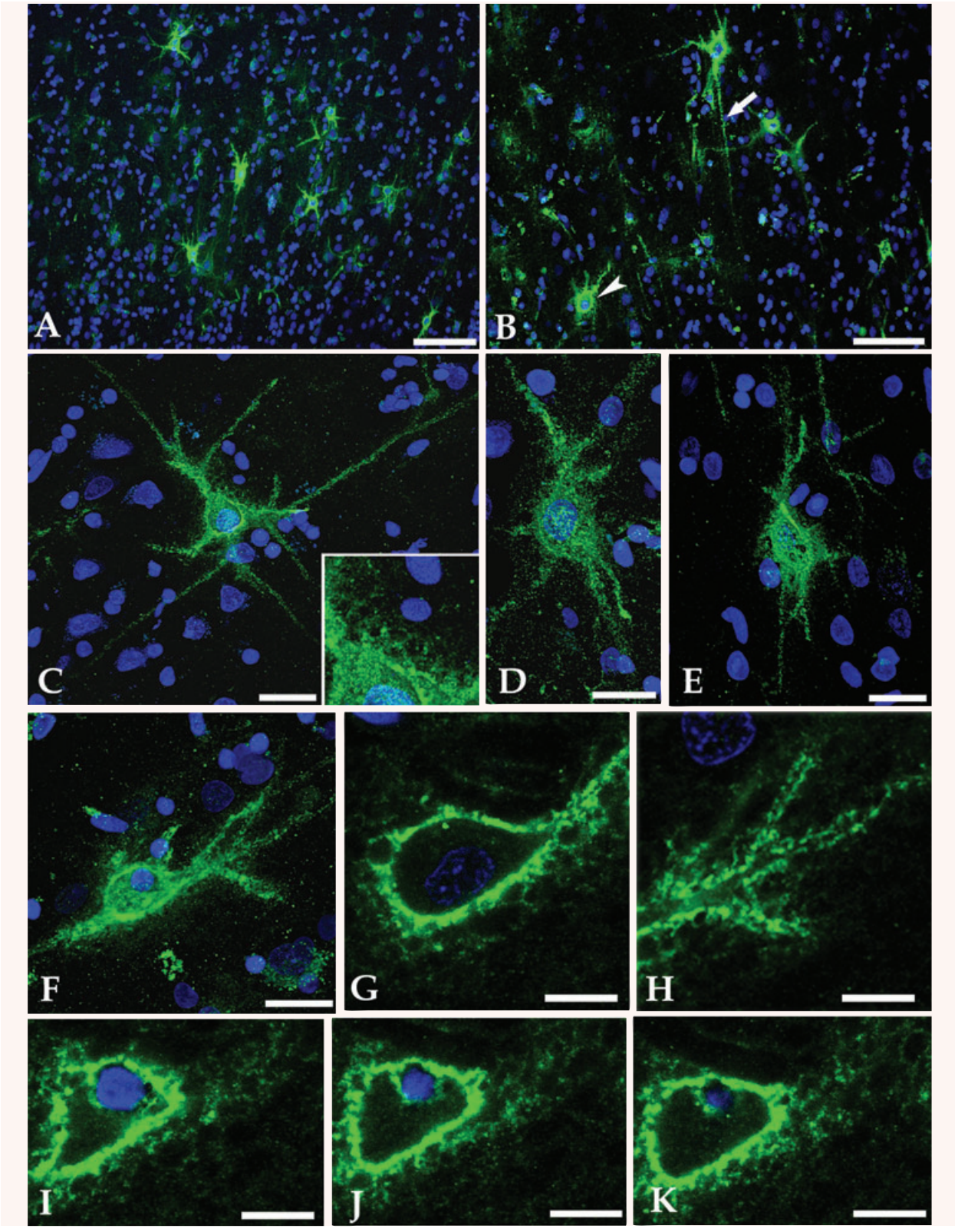

Fig. 7 Confocal laser microscopic images of Brodmann's area 6 sections following immunostaining with antibody 5D3. (**A**, **B**) Numerous neuronal cell bodies and processes are surrounded by aggrecan-containing PNNs in cortical layers III (**A**) and V (**B**); note in (**B**) a large polymorphous interneuron (arrowhead) and a neurite-like process (arrow) enwrapped by an aggrecan-rich matrix. (**C–E**) High magnification views of medium-sized polymorphous interneurons surrounded by aggrecan deposits forming a continuous PNNs 'coat'; note (*inset* in **C**) the aggrecan honeycomb-like halo. (**F**) A projection image of a coated polymorphous interneuron and (**G–K**) enlarged pictures of single optical planes of the same neuron; it is possible to appreciate the continuous aggrecan 'coat' surrounding the neuronal soma (**G)**, dendritic processes (**H**), and a perineuronal satellite cell (**I–J**); note (in **G–K**) how aggrecan deposits form honeycomb-like structures in the matrix close to the continuous aggrecan 'coat'. Counterstaining with the nuclear tracer TO-PRO-3. Magnification bars: **A**, **B**, 100 μm; **C–F**, 20 μm; **G–K,** 10 μm.

interneurons, as well as clusters of larger, polymorphous interneurons (Fig. 5A, F and G).

The aggrecan staining pattern observed with our antibody 5D3 in Brodmann's area 6 was compared by double immunolabelling on vibratome sections either with lectin WFA or with the reference antibody r-aggrecan. The double immunolabellings confirmed that PNNs containing aggrecan isoform(s) recognized by antibody 5D3 were restricted to a subpopulation of cortical neurons and that this antibody disclosed a greater number of PNNs compared to both WFA and the r-aggrecan antibody (Fig. 6A–F). The number of neurons surrounded by WFA PNNs, r-aggrecan and 5D3, together with the number of WFA/5D3 and r-aggrecan/5D3 co-localizations, were quantitatively evaluated by morphometry on a total cortical area of about 12.4 mm^2 (for WFA/5D3) and 11.2 mm^2 (for r-aggrecan/5D3). The results indicated that a limited number of 5D3-stained neurons was stained by WFA (14.9% $\pm$ 3.0%), whereas almost all WFA PNNs were also reactive to 5D3 (99.4% $\pm$ 0.6%). Despite some coincident staining of aggrecan 5D3 and r-aggrecan (99.8% $\pm$ 0.5%), a greater number of PNNs was revealed by our antibody 5D3 (84.4% $\pm$ 4.7%). These data suggest that antibody 5D3 detects aggrecan isoform(s) assembling a large subset of cortical neuron PNNs, whereas the reference antibody largely matches the staining pattern of our antibodies belonging to cluster 3.

Detailed analysis of aggrecan-containing PNNs and their relationships with synaptic boutons and astrocytic processes

To unveil the detailed features of aggrecan-containing PNNs, their precise spatial arrangement and their connections with nerve terminals and glial cell processes, we carried out a high-resolution laser confocal microscopical analysis on thicker vibratome sections single- and double-labelled with antibody 5D3 and antibodies to synaptophysin or GFAP. Through this approach we were able to confirm the lack of significant deposition of aggrecan isoform(s) detected by antibody 5D3 in cortical layer I. Conversely, a greater number of finer 5D3-aggrecan PNNs interspaced between denser ones was highlighted throughout cortical layers II–VI, in which aggrecan-decorated neuronal processes were also evident at considerable distances from the neuronal cell bodies from which they originated (Fig. 7A–E). Additional peculiar traits of aggrecan-containing PNNs were observed around the cell body of medium-large sized polymorphous interneurons of layers V and VI. In fact, some of these neurons appeared to be surrounded by aggrecan deposits forming a continuous 'coat' rather than exhibiting the typical PNN mesh-like appearance (Fig. 7C and F–K). Comprehensive images of the complete aggrecan-containing neuronal envelope were obtained by analysing both single optical planes and three-dimensional reconstructions of confocal projections, stacks of single optical planes (Figs. 7G and S4; Movie S1). Through these it was possible to reveal a honeycomb-like deposition of the aggrecan matrix around and along the dense PNN coating, suggestive of aggrecan containing boundaries of ECM encompassing pre-terminal nerve fibres (Figs. 7C, F–K and S4; Movie S2). These analyses further highlighted the presence of perineuronal satellite cells completely embedded within the aggrecan 'coat' (Figs. 7F, I–K and S4 and S5; Movies S1 and S2).

Detailed analysis of thicker sections double-labelled with antibody 5D3 and antibodies to synaptophysin – an integral membrane glycoprotein of the synaptic vesicles – demonstrated a number of synaptic boutons in contact with the aggrecan-containing PNNs (Fig. 8A). Views of single optical planes revealed the finer details of synaptophysin-containing boutons regularly alternated with aggrecan deposits around neuronal cell bodies and processes (Fig. 8B–D). Sections double-labelled with antibodies 5D3 and anti-GFAP highlighted an intricate pattern of astrocyte processes surrounding the neurons provided with aggrecan-rich PNNs (Fig. 8E) and terminating on the surfaces of these neurons, in close contact with the aggrecan deposits (Fig. 8F–H). Thus, aggrecan-containing matrices seemed to be interposed between neuronal processes, astrocytic processes and their terminals in contact with cell somas.

Differential association of aggrecan-containing PNNs with distinct classes of cerebral cortical neurons

We next sought to better characterize the classes of cortical neurons surrounded by aggrecan-containing PNNs. To this end, we employed a similar laser confocal microscopic approach, in this case entailing double immunolabelling of the sections with antibody 5D3 and either antibodies to the neurotransmitter Glu,

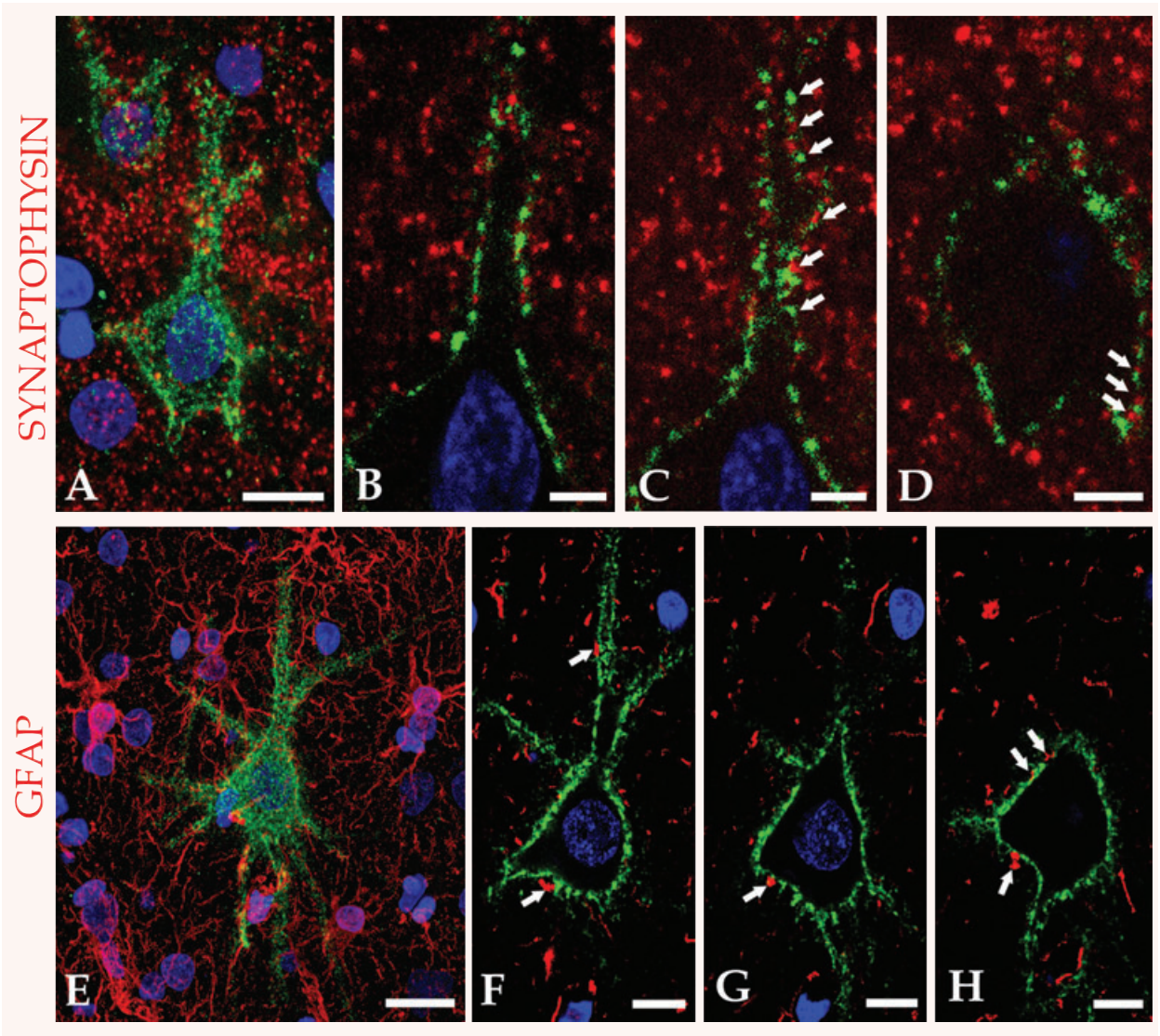

Fig. 8 Confocal laser microscopy images of sections through Brodmann's area 6 double-labelled for aggrecan with antibody 5D3 and synaptophysin (**A**–**D**) or GFAP (**E**–**H**). (**A**–**D**) On the projection image (**A**), aggrecan meshes and nerve terminals are tightly intermingled on the neuronal soma and dendrite surfaces. (**B**–**D**) show single optical planes of (**A**) highlighting details of aggrecan-deposits close to synaptic boutons on the primary dendrite (**B**; arrows in **C**) and cell soma (arrows in **D**). (**E**–**H**) On the projection image (**E**), the $GFAP^{+}$ astrocyte processes form a dense perineuronal network which penetrates the aggrecan-rich PNN; (**F**–**H**) show single optical planes of (**E**) evidencing processes in close contact with the aggrecan envelope (arrows). Counterstaining with the nuclear marker TO-PRO-3. Magnification bars: **A**, 15 μm; **B**–**D**, 5 μm; **E**, 20 μm; **F**–**H**, 10 μm.

adopted as a marker for pyramidal neurons, or antibodies against each of the Ca^{2+}BPs, calbindin, calretinin and parvalbumin, that have been demonstrated to specifically identify different subclasses of GABAergic interneurons. Stained sections were subjected to a semi-quantitative morphometric evaluation of the number/class of cortical neurons provided with aggrecan-rich PNNs. The results demonstrated that in a cortical area of 10.8 mm^2, 16.2% ± 5.8% of Glu-reactive pyramidal neurons that localized within cortical layers III, V and VI were provided with aggrecan-containing PNNs (Fig. 9A–C), whereas on the same area 28.8% ± 6.9% of interneurons, revealed by their reactivity for Ca^{2+}BPs, had these PNNs (Fig. 9D–F). Subsequently, the subclasses of cortical interneurons with associated aggrecan nets were revealed by double immunolabellings with antibody 5D3 and the individual interneuron markers parvalbumin, calbindin and calretinin. In cortical layer III, aggrecan-containing PNNs were consistently

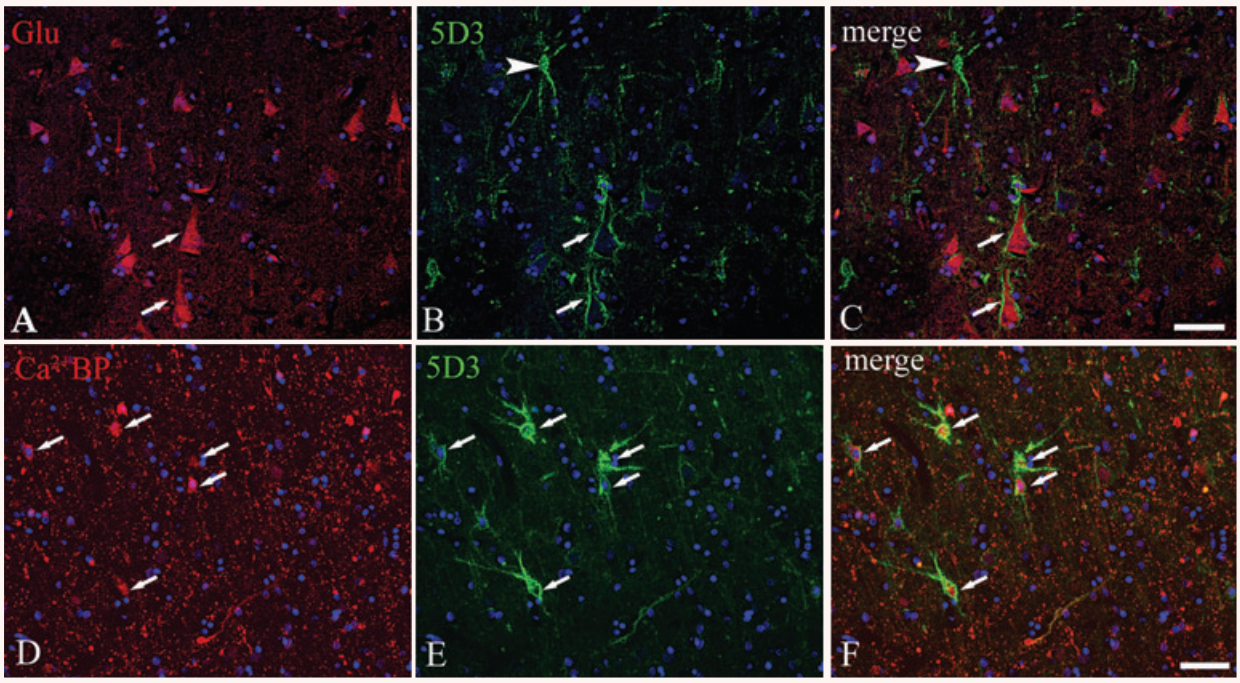

Fig. 9 Confocal laser microscopic images of sections through Brodmann's area 6 double-labelled for aggrecan with antibody 5D3 and either antibodies to glutamate (Glu; **A–C**) or to a combination of the three calcium binding proteins calbindin, calretinin and parvalbumin (Ca^{2+}BPs; **D–F**). (**A–C**) A cluster of pyramidal Glu^{+} neurons in cortical layer V (**A**), some of which are provided with aggrecan-rich PNNs (arrows, **A–C**); coincidently a Glu^{-} interneuron is revealed by an aggrecan-rich PNN (arrowhead in **B**, **C**). (**D–F**) Numerous interneurons revealed by Ca^{2+}BPs immunolabelling (**D**) show well-delineated aggrecan-rich PNNs (arrows; **E**, **F**). Counterstaining with the nuclear marker TO-PRO-3. Magnification bars: 100 μm.

associated with parvalbumin-expressing interneurons (Fig. 10A), whereas a few parvalbumin interneurons showed faint aggrecan PNNs in layers V and VI, while aggrecan deposits appeared to be only rarely associated with these neurons in layers II and IV. The total percentage of parvalbumin-positive interneurons associated with aggrecan-rich PNNs was estimated to be 65.0% ± 8.8% (Fig. 10B). A smaller fraction of calbindin-positive neurons was associated with aggrecan-containing PNNs in layers II and III (11.2 ± 4.4%; Fig. 10C and D). Finally, aggrecan-rich PNNs were never seen in association with calretinin-expressing interneurons residing within the different cortical layers (Fig. 10E and F).

Discussion

PNNs have recently been demonstrated to contribute to the stabilization of synaptic contacts during critical periods of brain development [7, 43–46] and in the adult brain. Apart from their implication in the maintenance of the tissue architecture and neuroprotection, they are also thought to provide a buffering microenvironment around neurons [47–50]. Lectican-type PGs are vital components of the CNS ECM [8, 11, 51] and primary elements of PNNs. In these structures, chondroitin sulphate chains attached to the different integral PGs seem to act as inhibitors of synaptogenesis, thereby mediating the stabilization effect of PNNs on synapses but at the same time hampering regenerative processing requiring dynamic modulation of synaptogenesis [44, 52–54]. The relative distribution of PGs in PNNs is therefore a subject of particular interest and has been previously investigated in a wealth of animal species, including chick, mouse, rat and cat [18–20, 22, 55–58]. Detailed information is also available concerning the glycan composition of PNNs in the rat CNS [23, 33, 59, 60]. Conversely, little is known about the structural and molecular composition of PNNs in the cerebral cortex of the human adult brain, nor how the assembly of these neuron-associated structures relates to neuronal function. This work makes a contribution to this problem by providing the first description of the distribution of aggrecan isoforms in Brodmann's area 6 and how their structural organization and differential association with subsets of neurons may define novel neuronal classes.

In the avian CNS the presence of aggrecan in telencephalic regions of the brain has previously been shown, and the synthesis of this PG by isolated neurons/neuronal precursors in culture confirmed [26, 32]. Aggrecan expression has also been documented

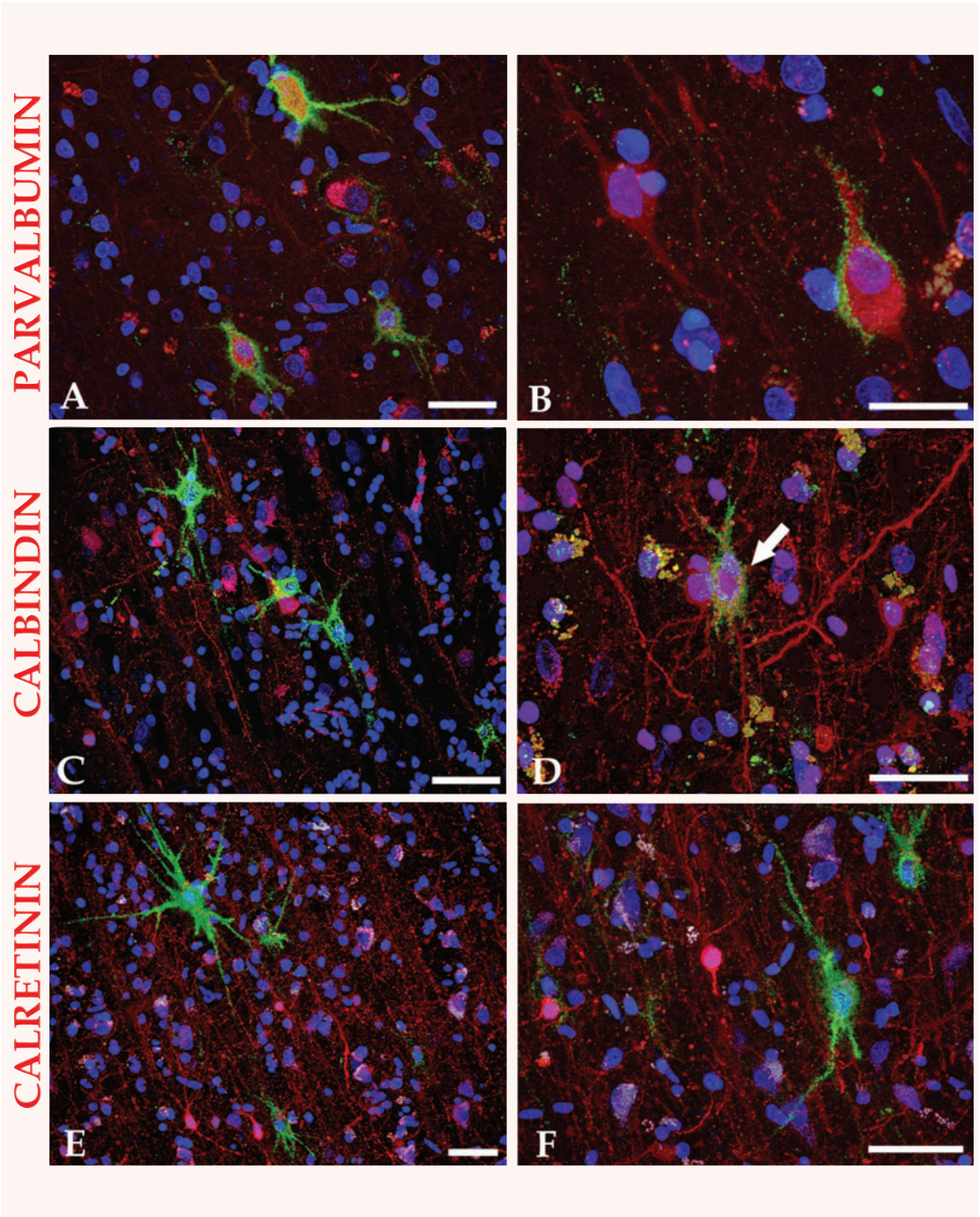

Fig. 10 Confocal laser microscopy images through Brodmann's area 6 double-labelled for aggrecan with antibody 5D3 and parvalbumin (**A**, **B**), calbindin (**C**, **D**), or calretinin (**E**, **F**). (**A**, **B**) Medium-sized parvalbumin-positive neurons of cortical layer III are surrounded by PNNs with various degrees of aggrecan deposition (**A**); two parvalbumin-positive neurons, one of which is associated with aggrecan PNN in cortical layer V (**B**). (**C**, **D**) Cortical layer III rich in calbindin-positive neurons not associated with aggrecan-rich PNNs (**C**); in this layer medium-sized calbindin interneurons associated with aggrecan PNN are only rarely recognizable (arrow in **D**). (**E**, **F**) Medium-sized calretinin-positive interneurons not surrounded by aggrecan PNNs, together with larger calretinin-negative interneurons associated with aggrecan PNNs. Counterstaining with the nuclear marker TO-PRO-3. Magnification bars: **A**, 30 μm; **B**, 20 μm; **C**, **D**, **F**, 50 μm; **E**, 100 μm.

in the mammalian CNS, where it has been suggested to be linked to different classes of neurons [12, 17, 22, 23, 31, 33, 61–63]. The use of antibodies Cat-301, Cat-315 and Cat-316, raised against feline chondroitin sulphate PGs and recognizing PGs of variable sizes compatible with those of neurocan and brevican, has provided some insights into the composition of PNNs in different areas of the CNS in a variety of species [17, 33, 43, 64], and significant information about the expression pattern of these lecticans in rodent CNS has also been obtained [23, 33]. However, although previous *in situ* hybridizations have highlighted aggrecan transcription in mammalian CNS neurons [33], the precise pattern of aggrecan isoform in the human CNS has remained undefined.

Our transcriptional analysis reveals that the adult human CNS expresses all aggrecan alternatively spliced isoforms present in cartilage and thus suggests that both ECM and PNNs may contain a wide spectrum of aggrecan protein variants. To gain a thorough description of the aggrecan isoforms expressed in the human cerebral cortex we made use of a panel of anti-human aggrecan antibodies that recognizes core protein-associated epitopes capable of distinguishing different aggrecan isoforms. While some of these antibodies were found to react with epitopes within defined aggrecan domains, other recognized epitopes were of a secondary or tertiary structural nature. Conformation-dependency of antibody reactivity may be one of the reasons for the differences in immunoblotting patterns observed between the aggrecan variants detected by our antibodies in the human brain and those previously reported for aggrecan glycoforms in the CNS of other mammals, including that of the cat, previously examined with anti-glycan moiety antibodies. Based upon a comparison between the molecular sizes and banding patterns of the putative aggrecan-like PGs detected in these previous studies and those detected by us, it seems possible that these previous investigations may have detected different subsets of aggrecan variants, distinguishable from the ones identified in this study. Alternatively, feline and human brain aggrecan variants may be intrinsically different, or differently distributed in the different brain regions of these species.

Some of our antibodies showed some reactivity with fragments corresponding to the GAG linkage region of shark cartilage, suggesting that they may be directed against this moiety [64]. At least four of the antibodies in our panel seemed to recognize epitopes shared by human and bovine cartilage aggrecans, and to some extent aggrecans from other species (but not other types of PGs), suggesting that they are directed against highly conserved sequences/structural features of aggrecan. A fairly incontrovertible proof of the fact that some of the antibodies of the panel reacted with structural epitopes was afforded by the failure of these antibodies to react with proteolytic fragments of aggrecan or recombinant fragments encompassing either the *C*-terminal G3 domain or the N-terminal G1-IGD-G2 segment.

Our comprehensive analysis of the aggrecan distribution in the adult human cerebral cortex provides the first evidence of aggrecan expression in the human cerebral cortex PNNs and corroborates recent observations in other mammals, including feline brain. However, striking differences could be noted when comparing aggrecan variant distribution in human brain with that seen in other mammals. In the human brain, aggrecan PNNs were present within all layers of the cortex except layer I, where aggrecan was absent from the interstitial matrix. The biological significance of this phenomenon is not clear, but may be associated with the different developmental origin of the neurons composing layer I [65] and with compositional differences in the matrix deposited in this region. On the other hand, in partial agreement with findings in other mammals, we observed that human cortical PNNs did not encompass keratan sulphate-bearing PGs, as shown by the fact that a specific antibody detecting this type of GAG chains exclusively localized keratan sulphates in the ECM of multiple cortical layers. This observation highlighted a potential crucial discrepancy in the glycanation pattern of human aggrecan isoforms deposited in the PNNs *versus* ECM of the CNS, as well as in aggrecan molecules assembled in cartilage matrices.

Previous morphological analyses of mammalian PNNs have emphasized a mesh-like organization of such structures, whereas our detailed analysis of human PNNs highlights the possibility that the accumulation of aggrecan isoforms on the neuronal surface creates a 'coat-like' structure which may also include perineuronal satellite cells. These may represent glial cells such as microglia and astroglia cells or possibly grey matter oligodendroglia cells classically described as perineuronal (perisomatic) satellite oligodendrocytes and typically located close to large neurons in the cerebral and cerebellar cortex [66–68]. Similarly, we noted that aggrecan densities were often found in close proximity to synaptic boutons and astroglia processes, suggesting that aggrecan-containing matrices may be determinant factors for the structuring of synapses and for mediating proper glial cells-neuron inter-relationships. Moreover, in the vicinity of aggrecan-rich PNNs, the interstitial matrix also containing aggrecan was more concentrated and aggrecan deposition in this matrix showed a gradient in which the denser aggrecan accumulations formed a honeycomb-like perineuronal 'halo' coinciding with the boundaries restricting pre-terminal nerve fibres.

When we compared the distribution pattern of aggrecan isoforms with the identification of interneurons, characterized by their high content of Ca^{2+}BPs, we found that only subsets of inhibitory interneuron subclasses were associated with aggrecan-rich PNNs, in a layer-specific manner. In fact, this association was more consistent and widespread through all cortical layers for parvalbumin-containing neurons, whereas the association with aggrecan-rich PNNs was less frequent and restricted to layers II and III for calbindin neurons, and completely absent for calretinin-containing neurons. Moreover, a subset of pyramidal neurons in layers III and V was found to be associated with aggrecan PNNs. The precise identity and function of these aggrecan-surrounded neuronal subsets remain to be established. One possibility, however, is that parvalbumin-positive neurons supplied with aggrecan-containing PNNs may correspond to the previously described subtype of fast spiking neurons characterized by Kv3.1 of the voltage-gated potassium channel [69–71]. Furthermore, since aggrecan was not found to be associated with calretinin neurons, it is suggested that aggrecan-rich PNNs may distinguish at least two classes of cerebral cortical neurons from the others, namely horizontal Cajal–Retzius neurons of cortical layer I and calretinin neurons residing within multiple cortical layers. The observed subset of pyramidal neurons associated with aggrecan PNN could represent a subpopulation of intracortical, long-range projection neurons.

In cartilage, aggrecan is known to contribute to tissue hydration, as well as to provide the necessary structural and mechanical stability of the tissue, by creating a polyanionic microenvironment with a high buffering capacity for cations. It is not known whether this is the case also in the CNS and what the physiological significance of creating such an inter-cellular microenvironment could be in this site. Overall, a protective role of PNNs has been shown in normal elderly brain and in neurodegenerative diseases [49, 72], and PNNs appear to be altered in some neurological diseases [73]. It remains to be clarified to what extent changes in the relative expression and distribution of aggrecan isoforms are involved in these morphological alterations, as well as to what extent aggrecan molecules may contribute to neuronal integrity. Deposits of different aggrecan variants in PNNs of defined neuronal subsets and distinct areas of the human cortex may contribute to the structural-functional diversity of these neuronal subpopulations, or may simply be a synthetic consequence of their diversified traits. A more precise determination of the functional traits of the aggrecan-surrounded neuronal subpopulations, along with a better understanding of the nature and structural-functional characteristics of these aggrecan isoforms, will shed further light on this issue.

Acknowledgements

We thank Carmen Capobianco for her excellent technical support and Dr. Karl Frei for human glioblastoma surgical samples (Department of Neurosurgery, University Hospital Zurich, Zurich, Switzerland). The work was supported by funds from the Italian Ministry of Education, University and Research (MIUR, PRONEURO and PRIN 2004); Fondazione Cassa di Risparmio di Puglia (FCRP, 2005); Progetto Strategico PS124 (Neurobiotech, 2006); Associazione Italiana Ricerca sul Cancro (AIRC, 2004–2007); Core Research for Evolutional Science and Technology of the Japan Science and Technology Corporation, Grants-in-aid for Scientific Research from the Ministry of Education, Science, Culture, and Sports of Japan, and Human Frontiers Science Program; intramural funds from the National Cancer Institute in Aviano and the University of Parma (2005–2008).

Supporting Information

The following supplementary material is available for this article:

Table S1 Demography of post-mortem tissue donors.

Table S2 Anti-aggrecan antibodies from R&D Systems, Inc.

Fig. S1 Representative global view of lectin WFA-reactive sugar moieties distribution in Brodmann's area 6 of the human cerebral cortex as observed in all the analysed brain samples. (**A–E**) Lectin WFA labels the neuropil ECM, the PNNs (arrows) and the wall of blood capillaries throughout all the cortical layers. Counterstaining with haematoxylin. Magnification bars: **A,** 400 μm; **B–E**, 100 μm.

Fig. S2 Representative image of tenascin expression in Brodmann's area 6 of the human cerebral cortex and in human glioblastoma. Tenascin-C is not found in the cortex (**A**), but shows diffuse staining in white matter ECM (**B**). For comparison, the glycoprotein is found to be abundantly expressed by neoplastic cells and neovascular structures of malignant glioblastoma lesions (**C**). Some tenascin-R can be seen in the cortex (**D**), but its expression is significantly poorer than in glioblastoma lesions (**E**). Counterstaining with haematoxylin. Magnification bars: **A–E**: 75 μm.

Fig. S3 Comparison between serial sections of the cerebral cortex Brodmann's area 6 stained with antibody 5D3 (**A**, **C**, **E**) and with antibodies against aggrecan isoforms pertaining to different clusters (**B**, **D**, **F**). Cluster 1 antibody 5D3 reveals numerous strongly reactive PNNs that are co-revealed in the adjacent section by cluster 2 antibody 7C9 (compare **A**, **B**; arrows), cluster 3 antibody 5G5 (compare **C**, **D**; arrows) and cluster 4 antibody 2G5 (compare **E**, **F**; arrows). Magnification bar: **A–F**, 100 μm.

Fig. S4 Single optical planes examined by confocal laser microscopy analysis of the neuron depicted in Fig. 7F. The images were digitalized at intervals of 2.5 μm through the *z*-axis of the section. Tangential planes to the neuron surface, *z*_05, *z*_10 and *z*_15, show a satellite cell (*sc*), the nucleus of the neuron (*N*) appearing in the subsequent optical planes from *z*_20 to *z*_35. Magnification bar: 25 μm.

Fig. S5 Single optical planes generated by confocal laser microscopy analysis of the neuron depicted in Fig. 7F. The chosen planes, *z*_07, *z*_10 and *z*_13, digitalized at intervals of 1.5 μm through the

z-axis of the section, show the detail of a neuron surrounded by an aggrecan-rich PNN (arrows) laying in close proximity to an aggrecan-PNN free neuron (arrowheads). Both neurons are associated with a satellite cell (*sc*), which in the case of the former neuron appears completely enwrapped in the aggrecan-rich coat. Magnification bar: 25 μm.

Movie S1 (3D Animation)

Three-dimensional reconstruction of a cortical neuron showing the distribution and continuity of the aggrecan-containing PNN revealed by antibody 5D3 and the presence of both aggrecan-coated and uncoated perineuronal satellite cells.

Movie S2 (Sequence of single optical planes)

The sequence of optical confocal planes illustrates the presence of aggrecan-rich honeycomb-like matrix fields in the vicinity of a neuron-associated PNN, a perineuronal aggrecan-embedded cell and finally, the neuronal cell soma.

This material is available as part of the online article from: http://www.blackwell-synergy.com/doi/abs/10.1111/j.1582-4934.2009.00694.x
(This link will take you to the article abstract).

Please note: Wiley-Blackwell are not responsible for the content or functionality of any supporting materials supplied by the authors. Any queries (other than missing material) should be directed to the corresponding author for the article.

References

1. **Golgi C.** Intorno all'origine del quarto nervo cerebrale e una questione istofisiologica che a questo argomento si collega. *Rend R Acc Lincei.* 1893; 2: 379–89.
2. **Golgi C.** Intorno alla struttura delle cellule nervose. *Boll Soc Med-Chir Pavia.* 1898; 1: 1–14.
3. **Ramón y Cajal S.** Las células de cilindro-eje corto de la capa molecular del cerebro. *Rev Trim Micrograf.* 1897; 105–27.
4. **Rutka JT, Apodaca G, Stern R, *et al.*** The extracellular matrix of the central and peripheral nervous systems: structure and function. *J Neurosurg.* 1988; 69: 155–70.
5. **Ruoslahti E.** Brain extracellular matrix. *Glycobiology.* 1996; 6: 489–92.
6. **Brückner G, Grosche J, Hartlage-Rübsamen M, *et al.*** Region and lamina-specific distribution of extracellular matrix proteoglycans, hyaluronan and tenascin-R in the mouse hippocampal formation. *J Chem Neuroanat.* 2003; 26: 37–50.
7. **Dityatev A, Schachner M.** Extracellular matrix molecules and synaptic plasticity. *Nat Rev Neurosci.* 2003; 4: 456–68.
8. **Rauch U.** Extracellular matrix components associated with remodelling process in brain. *Cell Mol Life Sci.* 2004; 61: 2031–45.
9. **Margolis RU, Lalley K, Kiang WL, *et al.*** Isolation of properties of a soluble chondroitin sulfate proteoglycan from brain. *Biochem Biophys Res Comm.* 1976; 73: 1018–24.
10. **Herndon ME, Lander AD.** A diverse set of developmentally regulated proteoglycans is expressed in the rat central nervous system. *Neuron.* 1990; 4: 949–61.
11. **Yamaguchi Y.** Lecticans: organizers of the brain extracellular matrix. *Cell Mol Life Sci.* 2000; 57: 276–89.
12. **Kabos P, Matudan H, Zandian M, *et al.*** Neural precursors express multiple chondroitin sulfate proteoglycans, including the lectican family. *Biochem Biophys Res Commun.* 2004; 318: 955–63.
13. **Schwartz NB, Domowicz M.** Proteoglycans in brain development. *Glycoconj J.* 2004; 21: 329–41.
14. **Cattaruzza S, Schiappacassi M, Ljungberg-Rose Å, *et al.*** Distribution of PG-M/versican variants in human tissues and de novo expression of isoform V3 upon endothelial cell activation and neoangiogenesis. *J Biol Chem.* 2002; 277: 47626–35.
15. **Aquino DA, Margolis RU, Margolis RK.** Immunohistochemical localization of a chondroitin sulfate proteoglycan in nervous tissue. II. Studies in developing brain. *J Cell Biol.* 1984; 99: 1130–9.
16. **Fujita SC, Tada Y, Murakami F, *et al.*** Glycosaminoglycan-related epitopes surrounding different subsets of mammalian central neurons. *Neurosci Res.* 1989; 7: 117–30.
17. **Zaremba S, Naegele JR, Barnstable CJ, *et al.*** Neuronal subsets express multiple high-molecular-weight cell-surface glycoconjugates defined by monoclonal antibodies Cat-301 and VC1.1. *J Neurosci.* 1990; 10: 2985–95.
18. **Bertolotto A, Rocca G, Canavese G, *et al.*** Chondroitin sulfate proteoglycan surrounds a subset of human and rat CNS neurons. *J Neurosci Res.* 1991; 29: 225–34.
19. **Köppe G, Brückner G, Härtig W, *et al.*** Characterization of proteoglycan-containing perineuronal nets by enzymatic treatments of rat brain sections. *Histochem J.* 1997; 29: 11–20.
20. **Murakami T, Murakami T, Su WD, *et al.*** Perineuronal nets of proteoglycans in the adult mouse brain are digested by collagenase. *Arch Histol Cytol.* 1999; 62: 199–204.
21. **Wegner F, Härtig W, Bringmann A, Grosche J, *et al.*** Diffuse perineuronal nets and modified pyramidal cells immunoreactive for glutamate and the GABA(A) receptor alpha1 subunit form a unique entity in rat cerebral cortex. *Exp Neurol.* 2003; 184: 705–14.
22. **Carulli D, Rhodes KE, Brown DJ, *et al.*** Composition of the perineuronal nets in the adult rat cerebellum and cellular origin of their components. *J Comp Neurol.* 2006; 494: 559–77.
23. **Deepa SS, Carulli D, Galtrey C, *et al.*** Composition of perineuronal net extracellular matrix in rat brain: a different disaccharide composition for the net-associated proteoglycans. *J Biol Chem.* 2006; 281: 17789–800.
24. **Brückner G, Morawski M, Arendt T.** Aggrecan-based extracellular matrix is an integral part of the human basal ganglia circuit. *Neuroscience.* 2008; 151: 489–504.
25. **Pantazopoulos H, Murray EA, Berretta S.** Total number, distribution, and phenotype of cells expressing chondroitin sulfate proteoglycans in the normal human amygdala. *Brain Res.* 2008; 1207: 84–95.
26. **Domowicz MS, Krueger RC, Li H, *et al.*** The nanomelic mutation in the aggrecan gene is expressed in chick chondrocytes

and neurons. *Int J Dev Neurosci.* 2000; 14: 196–201.

27. **Hennig AK, Mangoura D, Schwartz NB.** Large chondroitin sulfate proteoglycans of developing chick CNS are expressed in cerebral hemisphere neuronal cultures. *Brain Res Dev Brain Res.* 1993; 73: 261–72.
28. **John N, Krügel H, Frischknecht R, *et al.*** Brevican-containing perineuronal nets of extracellular matrix in dissociated hippocampal primary cultures. *Mol Cell Neurosci.* 2006; 31: 774–84.
29. **Domowicz MS, Mangoura D, Schwartz NB.** Aggrecan regulates telencephalic neuronal aggregation in culture. *Brain Res Dev Brain Res.* 2003; 143: 207–16.
30. **Domowicz MS, Sanders TA, Ragsdale CW, *et al.*** Aggrecan is expressed by embryonic brain glia and regulates astrocyte development. *Dev Biol.* 2008; 315: 114–24.
31. **Asher RA, Scheibe RJ, Keiser HD, *et al.*** On the existence of a cartilage-like proteoglycan and link proteins in the central nervous system. *Glia.* 1995; 13: 294–308.
32. **Domowicz MS, Mangoura D, Schwartz NB.** Cell specific-chondroitin sulfate proteoglycan expression during CNS morphogenesis in the chick embryo. *Int J Dev Neurosci.* 2000; 18: 629–41.
33. **Matthews RT, Kelly GM, Zerillo CA, *et al.*** Aggrecan glycoforms contribute to the molecular heterogeneity of perineuronal nets. *J Neurosci.* 2002; 22: 7536–47.
34. **Magro G, Schiappacassi M, Perissinotto D, *et al.*** Differential expression of mucins 1–6 in papillary thyroid carcinoma: evidence for transformation-dependent post-translational modifications of MUC1 in situ. *J Pathol.* 2003; 200: 357–69.
35. **Mazzucato M, Cozzi MR, Pradella P, *et al.*** Vascular PG-M/versican variants promote platelet adhesion at low shear rates and cooperate with collagens to induce aggregation. *FASEB J.* 2002; 16: 1903–16.
36. **Behrem S, Zarković K, Eskinja N, *et al.*** Distribution pattern of tenascin-C in glioblastoma: correlation with angiogenesis and tumor cell proliferation. *Pathol Oncol Res.* 2005; 11: 229–35.
37. **Fülöp C, Walcz E, Vaylon M, *et al.*** Expression of alternative spliced epidermal growth factor-like domains in aggrecan of different species. *J Biol Chem.* 1993; 268: 17377–83.
38. **Fülöp C, Cs-Szabò G, Glant TT.** Species-specific alternative splicing of the epidermal growth factor-like domain 1 of cartilage aggrecan. *Biochem J.* 1996; 319: 935–40.
39. **Dodge KJ, Coulter SN, Meek LM, *et al.*** A human-specific polymorphism in the coding region of the aggrecan gene. *J Biol Chem.* 1997; 272: 13974–9.
40. **Vilim V, Fosang AJ.** Characterization of proteoglycans isolated from associative extracts of human articular cartilage. *Biochem J.* 1993; 293: 165–72.
41. **de Waard P, Vliegenthart JFG, Harada T, *et al.*** Structural studies on sulfated oligosaccharides derived from the carbohydrate-protein linkage region of chondroitin-6-sulfate proteoglycans of shark cartilage. II. Seven compounds containing 2 or 3 sulfate residues. *J Biol Chem.* 1992; 27: 6036–44.
42. **Sugahara K, Ohi Y, Harada T, *et al.*** Structural studies on sulphated oligosaccharides derived from the carbohydrate-protein linkage region of chondroitin-6-sulfate proteoglycans of shark cartilage. 1. Six compounds containing 0 or 1 sulfate and/or phosphate residue. *J Biol Chem.* 1992; 267: 6027–35.
43. **Hockfield S, Kalb RG, Zaremba S, *et al.*** Expression of neural proteoglycans correlates with the acquisition of mature neuronal properties in the mammalian brain. *Cold Spring Harb Symp Quant Biol.* 1990; 55: 505–14.
44. **Pizzorusso T, Medini P, Berardi N, *et al.*** Reactivation of ocular dominance plasticity in the adult visual cortex. *Science.* 2002; 298: 1248–51.
45. **Carulli D, Rhodes KE, Fawcett JW.** Upregulation of aggrecan, link protein 1, and hyaluronan synthases during formation of perineuronal nets in the rat cerebellum. *J Comp Neurol.* 2007; 501: 83–94.
46. **McRae PA, Rocco MM, Kelly G, *et al.*** Sensory deprivation alters aggrecan and perineuronal net expression in the mouse barrel cortex. *J Neurosci.* 2007; 27: 5405–13.
47. **Brückner G, Brauer K, Härtig W, *et al.*** Perineuronal nets provide a polyanionic, glia-associated form of microenvironment around certain neurons in many parts of the rat brain. *Glia.* 1993; 8: 183–200.
48. **Celio MR, Blümcke I.** Perineuronal nets – a specialized form of extracellular matrix in the adult nervous system. *Brain Res Brain Res Rev.* 1994; 19: 128–45.
49. **Morawski M, Brückner MK, Riederer P, *et al.*** Perineuronal nets potentially protect against oxidative stress. *Exp Neurol.* 2004; 188: 309–15.
50. **Vitellaro-Zuccarello L, Bosisio P, Mazzetti S, *et al.*** Differential expression of several molecules of the extracellular matrix in functionally and developmentally distinct regions of rat spinal cord. *Cell Tissue Res.* 2007; 327: 433–47.
51. **Rauch U, Zhou XH, Roos G.** Extracellular matrix alterations in brains lacking four of its components. *Biochem Biophys Res Commun.* 2005; 328: 608–17.
52. **Murakami T, Ohtsuka A.** Perisynaptic barrier of proteoglycans in the mature brain and spinal cord. *Arch Histol Cytol.* 2003; 66: 195–207.
53. **Suzuki T, Akimoto M, Imai H, *et al.*** Chondroitinase ABC treatment enhances synaptogenesis between transplant and host neurons in model of retinal degeneration. *Cell Transplant.* 2007; 16: 493–503.
54. **Dityatev A, Brückner G, Dityateva G, *et al.*** Activity-dependent formation and functions of chondroitin sulfate-rich extracellular matrix of perineuronal nets. *Dev Neurobiol.* 2007; 67: 570–88.
55. **Hausen D, Brückner G, Drlicek M, *et al.*** Pyramidal cells ensheathed by perineuronal nets in human motor and somatosensory cortex. *Neuroreport.* 1996; 7: 1725–29.
56. **Yamada H, Fredette B, Shitara K, *et al.*** The brain chondrotin sulfate proteoglycan brevican associates with astrocytes ensheating cerebellar glomeruli and inhibits neurite outgrowth from granule neurons. *J Neurosci.* 1997; 17: 7784–95.
57. **Takahashi-Iwanaga H, Murakami T, Abe K.** Three-dimensional microanatomy of perineuronal proteoglycan nets enveloping motor neurons in the rat spinal cord. *J Neurocytol.* 1998; 27: 817–27.
58. **Costa C, Tortosa R, Doménech A, *et al.*** Mapping of aggrecan, hyaluronic acid, heparan sulphate proteoglycans and aquaporin 4 in the central nervous system of the mouse. *J Chem Neuroanat.* 2007; 33: 111–23.
59. **Bahia CP, Houzel JC, Picanço-Diniz CW, *et al.*** Spatiotemporal distribution of proteoglycans in the developing rat's barrel field and the effects of early deafferentation. *J Comp Neurol.* 2008; 510: 145–57.
60. **Galtrey CM, Kwok JC, Carulli D, *et al.*** Distribution and synthesis of extracellular matrix proteoglycans, hyaluronan, link proteins and tenascin-R in the rat spinal cord. *Eur J Neurosci.* 2008; 27: 1373–90.
61. **Oohira A, Matsui F, Matsuda M, *et al.*** Occurrence of three distinct molecular species of chondroitin sulfate proteoglycan in the developing rat brain. *J Biol Chem.* 1988; 263: 10240–6.

62. **Fryer HJ, Kelly GM, Molinaro L, *et al*.** The high molecular weight Cat-301 chondroitin sulfate proteoglycan from brain is related to the large aggregating proteoglycan from cartilage, aggrecan. *J Biol Chem.* 1992; 267: 9874–83.
63. **Popp S, Maurel P, Andersen JS, *et al*.** Developmental changes of aggrecan, versican and neurocan in the retina and optic nerve. *Exp Eye Res.* 2004; 79: 351–6.
64. **Cheng F, Heinegard D, Fransson LA, *et al*.** Variations in the chondroitin sulfate-protein linkage region of aggrecans from bovine nasal and human articular cartilages. *J Biol Chem.* 1996; 271: 28572–80.
65. **Marin-Padilla M.** Dual origin of the mammalian neocortex and evolution of the cortical plate. *Anat Embryol.* 1978; 152: 109–26.
66. **Ludwin SK.** The perineuronal satellite oligodendrocyte. A role in remyelination. *Acta Neuropathol.* 1979; 47: 49–53.
67. **D'Amelio F, Eng LF, Gibbs MA.** Glutamine synthetase immunoreactivity is present in oligodendroglia of various regions of the central nervous system. *Glia.* 1990; 3: 335–41.
68. **Ambrosi G, Virgintino D, Benagiano V, *et al*.** Glial cells and blood-brain barrier in the human cerebral cortex. *Ital J Anat Embryol.* 1995; 100: 177–84.
69. **Weiser M, Bueno E, Sekirnjak C, *et al*.** The potassium channel subunit KV3.1b is localized to somatic and axonal membranes of specific populations of CNS neurons. *J Neurosci.* 1995; 15: 4298–314.
70. **Härtig W, Derouiche A, Welt K, *et al*.** Cortical neurons immunoreactive for the potassium channel Kv3.1b subunit are predominantly surrounded by perineuronal nets presumed as a buffering system for cations. *Brain Res.* 1999; 842: 15–29.
71. **Adams I, Brauer K, Arèlin C, *et al*.** Perineuronal nets in the rhesus monkey and human basal forebrain including basal ganglia. *Neuroscience.* 2001; 108: 285–98.
72. **Brückner G, Hausen D, Härtig W, *et al*.** Cortical areas abundant in extracellular matrix chondroitin sulphate proteoglycans are less affected by cytoskeletal changes in Alzheimer's disease. *Neuroscience.* 1999; 92: 791–805.
73. **Belichenko PV, Miklossy J, Belser B, *et al*.** Early destruction of the extracellular matrix around parvalbumin-immunoreactive interneurons in Creutzfeldt-Jakob disease. *Neurobiol Dis.* 1999; 6: 269–79.